Czech Technical University in Prague

Faculty of Electrical Engineering

Department of Electrotechnology

Bachelor Thesis

Diagnosis of photovoltaic modules using alternate methods of measurement

Author: Meiirbek Nariman

Supervisor: Tomas Finsterle

Study program: Applied Electrical Engineering

Prague 2017

Czech Technical University in Prague
Faculty of Electrical Engineering

Department of Electrotechnology

BACHELOR THESIS ASSIGNMENT

First name and family name of student: **Meiirbek Nariman**

Study programme: Electrical Engineering, Power Engineering and Management
Specialisation: Applied Electrical Engineering

Title of Bachelor Project: **Diagnosis of photovoltaic modules using alternate methods of measurement**

Guidelines:

1. Process and describe the problematics of PV modules diagnostics with focus on Impedance Spectroscopy, Electroluminescence and Flash test measurement methods and influence of paralel rezistors .
2. Apply the methods mentioned above on the set of crystalline silicon PV modules.
3. Discuss the results in terms of comparing results.

Bibliography/Sources:

[1] Gray, Jeffery L. The Physics of the Solar Cell. A. Luque a S. Hegedus. Handbook of Photovoltaic Science and Engineering. Chichester : John Wiley & Sons, Ltd., 2003, 3.
[2] CHEVNIDHYA, D., K. KIRTIKARA a C. JIVACATE Dynamic Impedance Characterization of Solar Cells and PV Modules Based on Frequency and Time Domain Analyses. Trends In Solar Energy Research. Hough, T.P. New York: Nova Science Publishers, 2006, s. 21-45. ISBN 1-59454-866-8; LCCN: 2005034740.
[3]Taylor, N. (Ed.): Guidelinesfor PV PowerMeasurement in Industry, Italy: EuropeanComission, Joint Research Centre, Institute forEnergy. 2010-04. Cite 2011. ISBN: 978-92-79-15780-6.

Bachelor Project Supervisor: **Ing. Tomáš Finsterle**

Valid until the end of the summer semester of academic year 2017/2018

ČESKÉ VYSOKÉ UČENÍ TECHNICKÉ V PRAZE

ZADÁNÍ BAKALÁŘSKÉ PRÁCE

I. OSOBNÍ A STUDIJNÍ ÚDAJE

Příjmení: **Nariman** Jméno: **Meiirbek** Osobní číslo: **437908**

Fakulta/ústav: **Fakulta elektrotechnická**

Zadávající katedra/ústav: **Katedra elektrotechnologie**

Studijní program: **Elektrotechnika, energetika a management**

Studijní obor: **Aplikovaná elektrotechnika**

II. ÚDAJE K BAKALÁŘSKÉ PRÁCI

Název bakalářské práce:

Diagnosis of photovoltaic modules using alternate methods of measurement

Název bakalářské práce anglicky:

Diagnosis of photovoltaic modules using alternate methods of measurement

Pokyny pro vypracování:

1. Process and describe the problematics of PV modules diagnostics with focus on Impedance Spectroscopy, Electroluminescence and Flash test measurement methods and influence of paralel rezistors .
2. Apply the methods mentioned above on the set of crystalline silicon PV modules.
3. Discuss the results in terms of comparing results.

Seznam doporučené literatury:

[1] Gray, Jeffery L. The Physics of the Solar Cell. A. Luque a S. Hegedus. Handbook of Photovoltaic Science and Engineering. Chichester : John Wiley & Sons, Ltd., 2003, 3.
[2] CHEVNIDHYA, D., K. KIRTIKARA a C. JIVACATE Dynamic Impedance Characterization of Solar Cells and PV Modules Based on Frequency and Time Domain Analyses. Trends In Solar Energy Research. Hough, T.P. New York: Nova Science Publishers, 2006, s. 21-45. ISBN 1-59454-866-8; LCCN: 2005034740.
[3]Taylor, N. (Ed.): Guidelinesfor PV PowerMeasurement in Industry, Italy: EuropeanComission, Joint Research Centre, Institute forEnergy. 2010-04. Cite 2011. ISBN: 978-92-79-15780-6.

Jméno a pracoviště vedoucí(ho) bakalářské práce:

Ing. Tomáš Finsterle, katedra elektrotechnologie FEL

Jméno a pracoviště druhé(ho) vedoucí(ho) nebo konzultanta(ky) bakalářské práce:

Datum zadání bakalářské práce: **17.02.2017** Termín odevzdání bakalářské práce: **26.05.2017**

Platnost zadání bakalářské práce: do 7.9.2018

Podpis vedoucí(ho) práce | Podpis vedoucí(ho) ústavu/katedry | Podpis děkana(ky)

III. PŘEVZETÍ ZADÁNÍ

Student bere na vědomí, že je povinen vypracovat bakalářskou práci samostatně, bez cizí pomoci, s výjimkou poskytnutých konzultací. Seznam použité literatury, jiných pramenů a jmen konzultantů je třeba uvést v bakalářské práci.

Datum převzetí zadání | Podpis studenta

Declaration

I declare that I have wrote my Bachelor Thesis ''Diagnosis of photovoltaic modules using alternate methods of measurement'' on my own and I have used only cited literature and other professional sources.

In Prague …….. ……

Acknowledgement

I would like to express my appreciation to my supervisor Ing. Tomáš Finsterle, also Ing. Jan Kyncl for their help and support. Thank you for providing me the possibility to complete this bachelor thesis.

1 ABSTRACT

The bachelor thesis is about diagnostics of photovoltaic (PV) modules using alternate methods of measurement. Technologies are described with the focus on PV modules structure. The thesis contains from two basic parts: Theoretical and Practical. For measurement are used three different methods – Impedance Spectroscopy, Electroluminescence and Flash Test. For describing these methods are used two types of crystalline silicon: monocrystalline and polycrystalline.

2 INTRODUCTION

Nowadays solar energy, also known as photovoltaics (PV) is one of the most available energy in the market. In addition, we can call it flat photosensitive diodes. It can provide electricity to places, where is no electric grid connection. Renewable energy sources are becoming more popular, because costs of PV modules have decreased the last 5 years and in comparing with other energy sources, it has low pollution. Solar cells are made of materials, which are called semiconductors. PV generates direct current (DC) from these semiconductors when they are irradiated by photons. In addition, the main advantage of such solar cell is that it does not need recharging. Their lifetime can reach 20-30 years. [1]

Technologies of a solar energy can be characterized by active solar and passive solar. It depends on how they dispense or convert solar energy into solar power. Speaking about active solar, we mean PV systems, solar water heating and concentrated solar power. Passive one include light-dispersing properties and building orientation directly to the sun.

The most usable materials for PV cells are silicon (Si), GaAs, CdTe, $CuInSe_2$ etc. The PV cells are made from light-absorbing materials. When the cell is joined with a load, optically generated carriers create an electric current. [1] Sunlight is produced of particles called photons, which radiate from the sun. A photon, which have acceptable energy to hit Si atoms of the solar cell, makes electrons of the Si out if its orbit. Then these freely move electrons go into an electric circuit. This is due to an electrical imbalance in the cell, where the electrons will flow in the one direction.

Atoms of the Si are formed together in a tightly bounded structure. Some quantities of other elements squeezes into this structure and build up two types of Si: p-type, which are electron-hole pairs, and n-type, which has spare electrons. High intensity of sunlight gives us a stronger current.

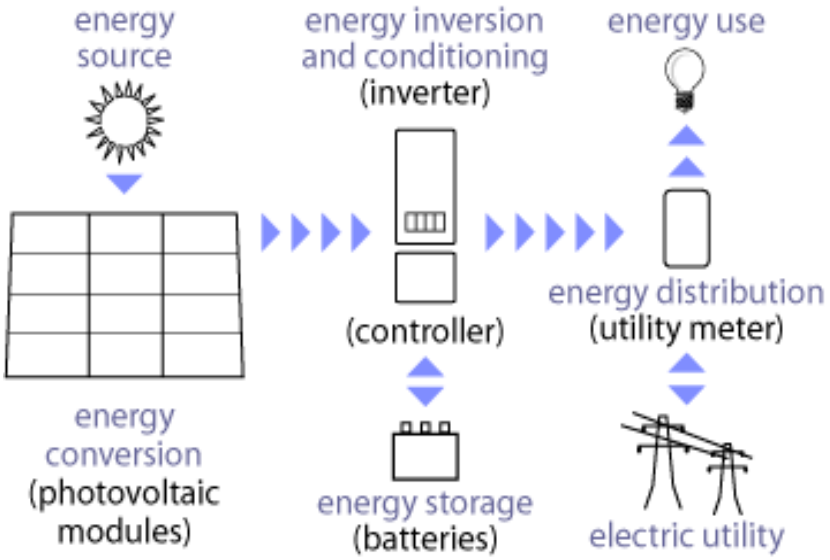

Figure 1: Components of PV system. [2]

This bachelor thesis is about crystalline silicon photovoltaic modules and their diagnostics using three different methods: Impedance Spectroscopy, Electroluminescence and Flash Test. By these

methods, we need to analyze the performance and find possible deviations against the standard specifications.

There are exists two types of measurement: indoor and outdoor. We focus only on indoor measurement, because in the case of outdoor it can be some problems with standard test conditions (STC). The STC are 25 ˚C, 1000 W/m^2 and AM 1.5 global spectrum. [3] It is useful for consumers to see how different PV modules works beneath the same conditions. However, they do not show the real operating conditions of PV devices. Saying indoor measurements, we mean flash test, electroluminescence and impedance spectroscopy. Electroluminescence is a photographic optical phenomenon, which can detect possible problems and defects of the solar cell. Because the human eyes do not have this ability. It is very important, because these defects can decrease the output power and efficiency of the solar cell. Electroluminescence is the consequence of radiative recombination of holes and electrons in a semiconductor with wide enough bandwidth to allow exit of the light. To determine dynamic parameters we can use impedance spectroscopy. The third measurement is Flash Test (or sun simulators). By this method, we measure the output performance of a solar PV module. Parameters of the module are measured using STC. Temperature is very necessary for PV module performance. When temperature increases the voltage output of each cell decreases and the current output of each cell a little bit increases, overall reducing the maximum power output in Watt.

Also, exists other alternating measurement techniques. For example, Time Domain Reflectometry (TDR) is a measurement, which is intended to figure out the characteristics of electrical lines by detecting reflected waveforms. This electronic device measures reflections along a conductor. By listening these reflections, it transmits an incident signal to the conductor. It has a same principle as a radar. The reflections are determined at the output or input to the TDR and plotted as a function of time.

3 THEORETICAL PART

3.1. Crystalline silicon PV cells

Crystalline silicon (c-Si) photovoltaics is the most popular and usable PV technology. 85-90% of the market is composed from c-Si. [8] It is the main semiconducting material, which is used for solar cell production. From c-Si PV cells are built PV modules, established from the microelectronics technology industry.

The most of c-Si are fabricated from silicon wafers and there are two types:

1) monocrystalline silicon (mono-Si) is a single large crystal

2) multicrystalline silicon (multi-Si) is solidified into small crystals

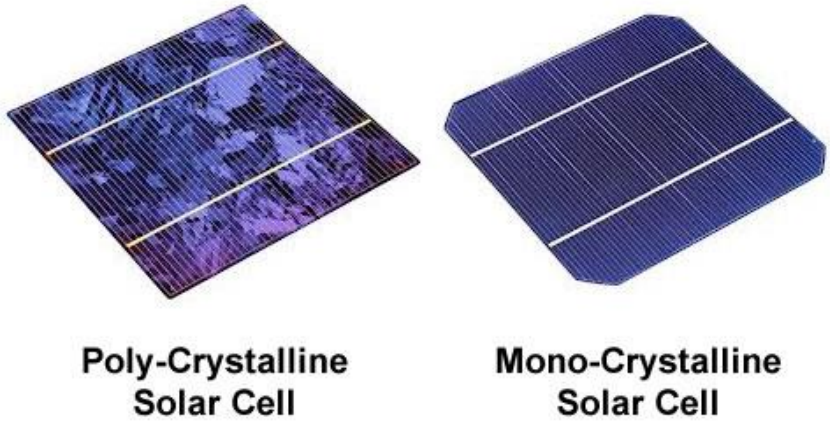

Efficiencies of these c-Si solar cells are approximately the same. For example, if we accept that area is up to 400cm^2, efficiency of the monocrystalline c-Si will be 18% and efficiency of the polycrystalline c-Si will be 17%. [3] Efficiency, like a fill factor, series and shunt resistances can be calculated from I-V curve and shows performance of a PV cell.

To make a c-Si solar cell wafers of high-purity silicon are “doped” with various impurities and fused together. Finally, we get a structure, which creates a pathway for current within and a between the solar cells. Usually monocrystalline wafers have better parameters of a material, but in comparing with multicrystalline, they have higher costs. It has an ordered crystal structure and every atom is ideally situated in the right place. In the case of multicrystalline, production techniques are more simple and cheaper. Because of grain boundaries, the quality of material is lower. These grain boundaries cut down performance of a solar cell by reason of blocking flows of carriers. [4]

The Si wafer of the cell consist of the electrical contacts, which are covered with an anti-reflective coating. This coating absorbs the light from the sun more profitably. Electrical contacts arrange the connection between the external load and the semiconductor material.

A direct bandgap of the c-Si is about 3eV and an indirect bandgap is 1.17eV.

To obtain a higher current we connect solar cells in parallel, and in series to obtain a higher voltage. Standard criterions of a single solar cell are 0.5V, 30 mA/cm^2. Typically, area of one cell

is 156mm x 156mm. If we connect 6 such solar cells in series, we obtain 3V output voltage (0.5V*6 = 3V). Important parameters, which defines a solar cell are Short-circuit current (I_{SC}), Open-circuit voltage (V_{OC}), Fill factor (FF), Series and Shunt resistances (R_S, R_{SH}) and Maximum power point (P_m). [3]

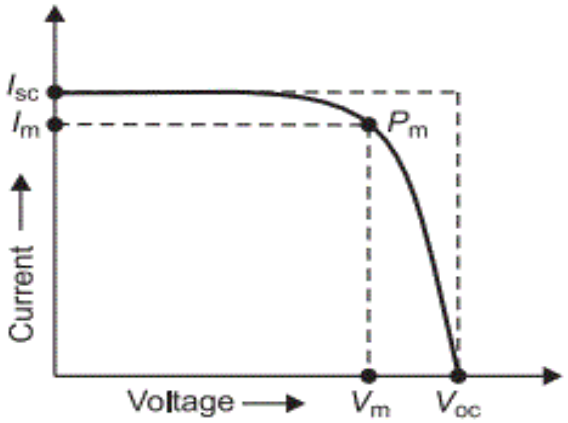

Figure 3. I-V characteristics of a solar cell.

I_{SC} is the current passes through the cell when the voltage across is 0.

V_{OC} is the maximum available voltage from a cell, obtained at 0 current. There is no load connection of the terminals of the modules.

FF is the power at the **P_m** divided by the **I_{SC}** and **V_{OC}** :

$$FF = \frac{V_{mp} I_{mp}}{V_{OC} I_{SC}} \tag{1}$$

R_{SH} is mainly located inside the structure of the solar cell and means defects.

R_S shows ohmic losses inside the solar cell.

P_m is the solar cell's maximum power production.

$$P_m = V_{mp} I_{mp} \tag{2}$$

or we can also calculate **P_m** using this formula:

$$P_m = V_{OC} I_{SC} FF \tag{3}$$

Efficiency of a solar cell can be calculated by this formula:

$$\eta = \frac{V_{OC} I_{SC} FF}{G A_C} \tag{4}$$

where: G – incident solar radiation, A_C – area of a solar cell.

There exist two main measurement conditions: under dark and under illumination. (Fig.4). Measuring in the dark is more effective, because under illumination small fluctuations in the intensity of the light gives us noise and makes production more difficult. A solar cell under dark

condition is a flat diode and IV measurement produces exponential curve. V_{OC} and I_{SC} indicates illuminated one. The current crossing the junction is roughly uniform and travels from the emitter to the contacts. [4]

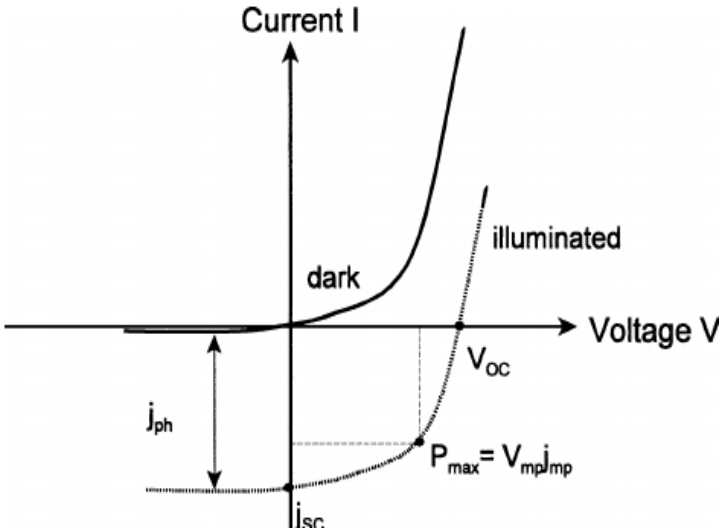

Figure 4: A solar cell under dark and under illumination.

Here is temperature dependent I-V measurement of c-Si. Measured by two multimeters, thermometer, hot plate and resistance decade.

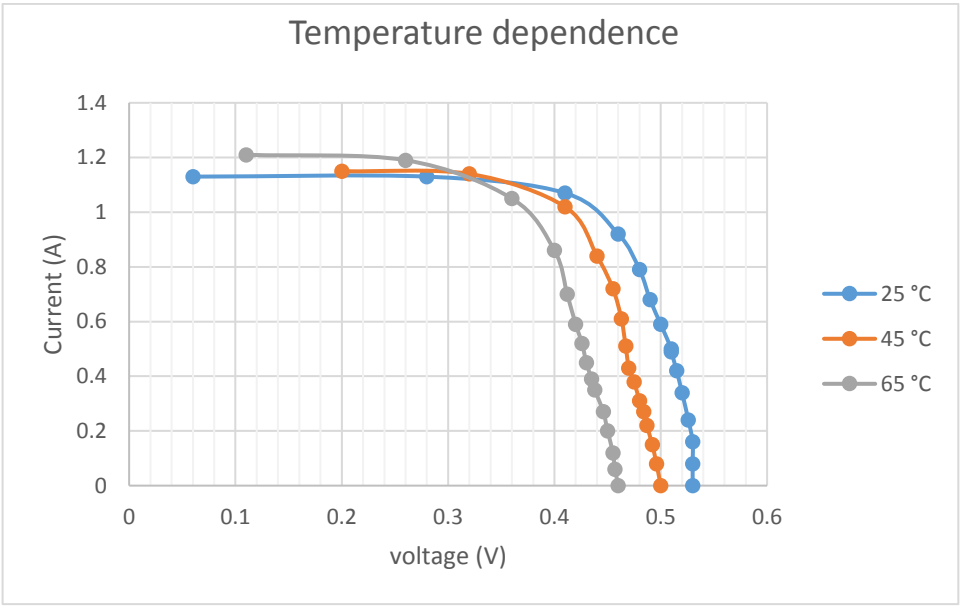

Figure 5: Temperature dependent I-V measurement of c-Si.

When temperature increases, voltage decreases. At zero load, current slightly increases. At the minimum temperature 25°C, we have the maximum open-circuit voltage V_{OC} and the minimum short-circuit current I_{SC}. At the maximum temperature 65°C, we have the minimum V_{OC} and the maximum I_{SC}.

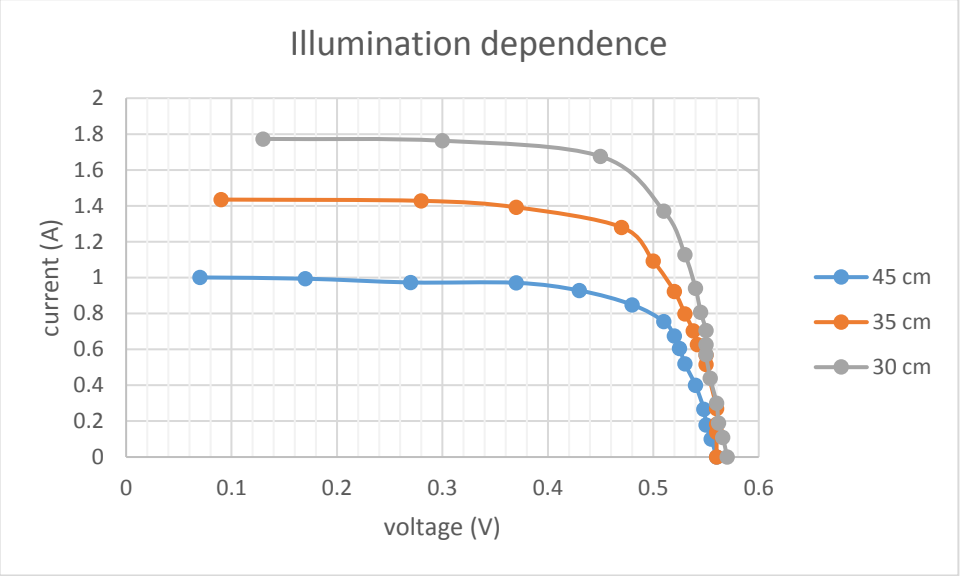

Figure 6: Illumination dependent I-V measurement of c-Si.

When distance is closer, we have more irradiance and voltage slightly increases. At zero load, current changes a lot. At the closest distance 30 cm, we have the maximum values of open-circuit voltage V_{OC} and short-circuit current I_{SC}. At the furthest distance 45 cm, we have the minimum values of V_{OC} and I_{SC}.

In practice, PV systems do not operate under STC, it always have some differences. Using of knowledge about temperature and irradiance dependences are very helpful.

3.2. Crystalline silicon PV modules

A single cell cannot give us required useful output for production. Therefore, to increase the level of power of a PV system, we connect number of such PV solar cells (commonly 36). They are coupled together to make a commercially available PV module. One PV module can be appraised from 3W to 250W.

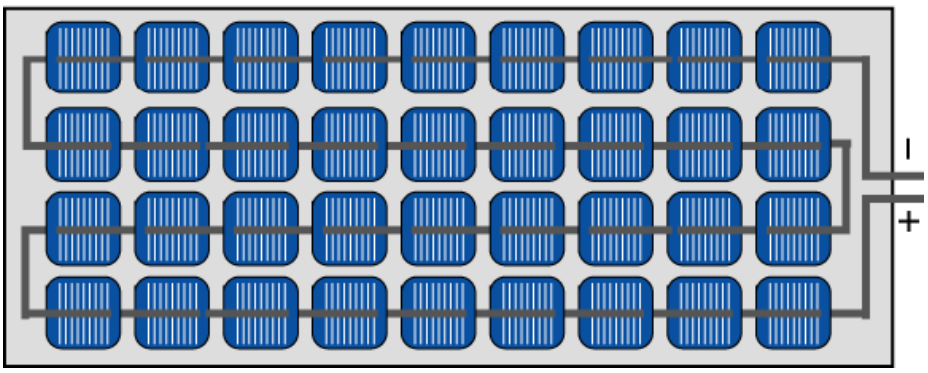

Figure 7: Series connected PV cells. [4]

Modules containing 36 cells in series gives us V_{OC} = 21V under STC and V_{mp} = 17V or 18V. Usually we choose a PV module with voltage, which is compatible with a 12V battery. [4]

The most important effects of PV modules are the temperature, failure modes and losses. [4]

We can connect PV cells in series or in parallel (Fig.8, 9). By multiplying the power of a single cell and the number of them, we can obtain power of the module. The module voltage is the voltage of the single cell times the number of series-connected cells, and current of the module is the current of the single cell times the number of paralleled cells.

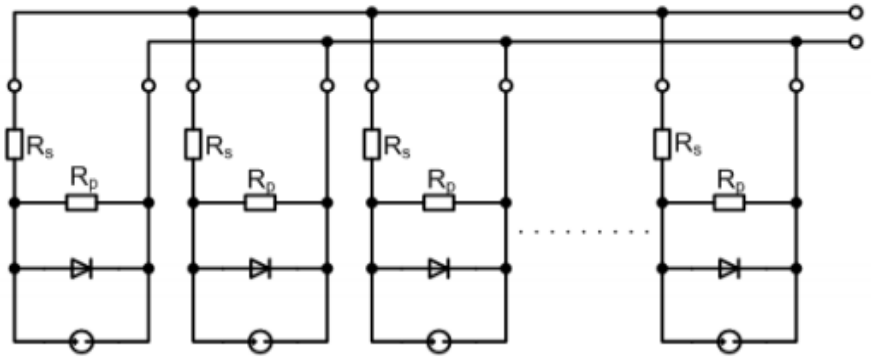

Figure 8: Series connection of PV cells. [3]

In this case, voltages sum up and all cells have the same current I_{mp}.

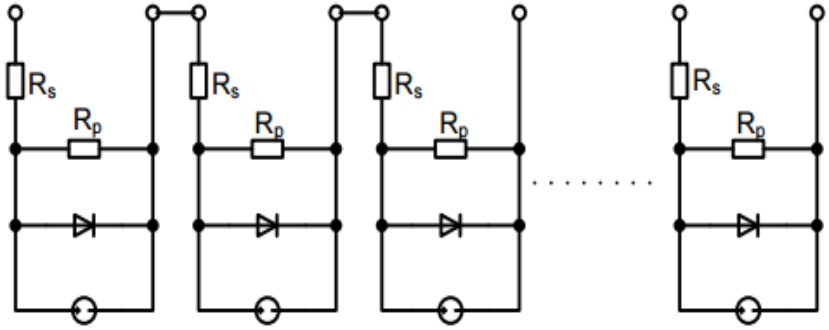

Figure 9: Parallel connection of PV cells. [3]

In this case, currents sum up and all cells have the same voltage V_{mp}. In both cases, we have efficiency losses because of partial shading.

On the figure below, we have two different modules: 72 solar cells connected in series and 72 solar cells connected in series with 8 by-pass diodes. Strings are oriented parallel to the window. 72 solar cells with 8 by-pass diodes more effectively preserve the power. From the graph, we can see that 72 solar cells with 8 by-pass diodes has better characteristics than solar cells without any diode.

Connection of by-pass diode is parallel, but it has opposite polarity to a solar cell. In the case of standard operation, each cell will be forward biased and therefore the by-pass diode will be reverse biased and will be an open circuit. It has no effect on output.

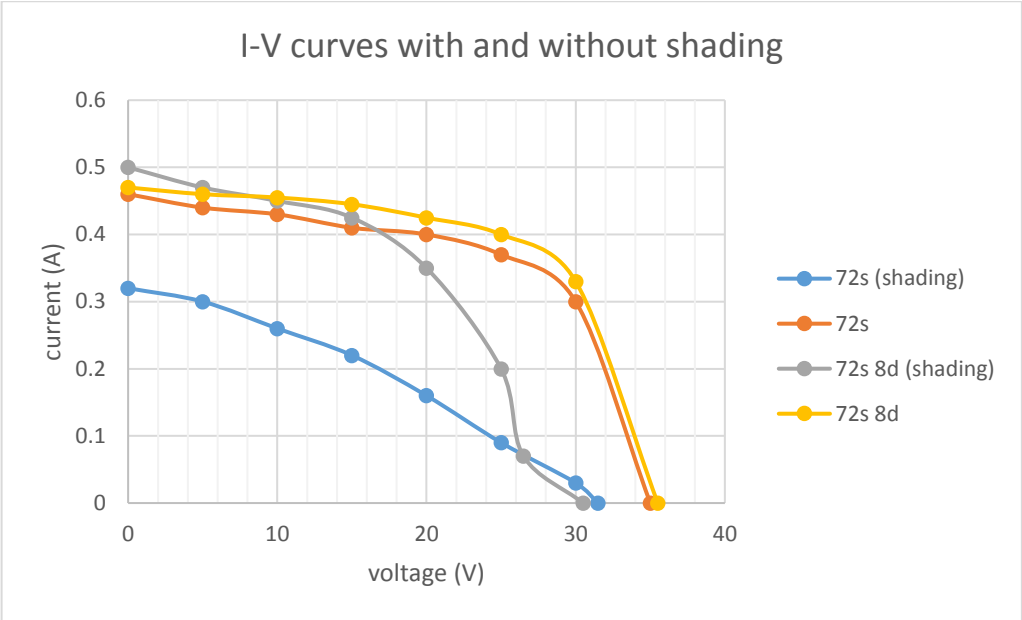

Figure 10: I-V curves with and without shading for two different modules.

In ideal case, there must be one diode across each solar cell, but it is very expensive. To solve this problem we can use only one by-pass diode for 12-24 solar cells, which are connected in series.

We can perform illuminated I-V measurement by X-Y plotter and potentiometer:

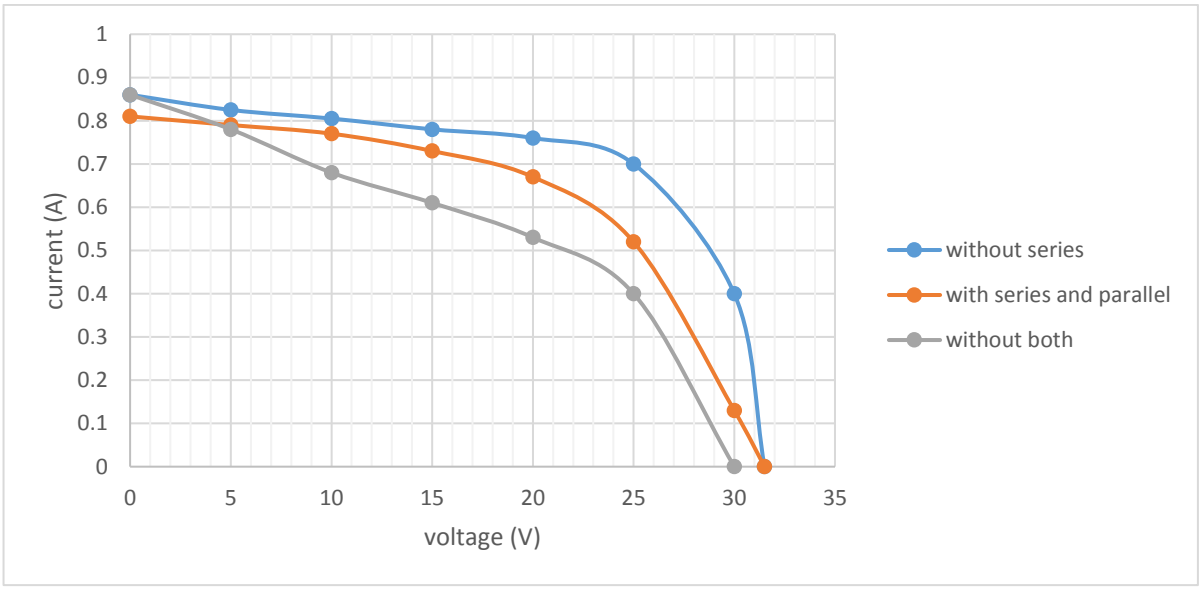

Figure 11: Illuminated I-V measurement of c-Si with and without supplied resistor on series and parallel.

We have two common points between the resistor in parallel and without any resistor. They have the same current value. In addition, between the resistor in both series and parallel and the resistor without series connection. They have the same voltage value. From this graph, we have the opportunity to indicate and calculate short-circuit resistor and open-circuit resistor. With both series and parallel connection, we have the maximum value of these two resistors.

Operating temperature of the PV modules depends on the ambient temperature and construction of the module. Difference between ambient and cell temperatures is proportional to irradiance G and total thermal resistance r_{th}.

$$T_c = T_a + r_{th}G \tag{5}$$

Nominal Operating Cell Temperature (NCOT) is the cell temperature at the ambient temperature 20 °C, irradiance G = 0.8 kWm^{-2}. [4]

3.3. Model of static PV cells

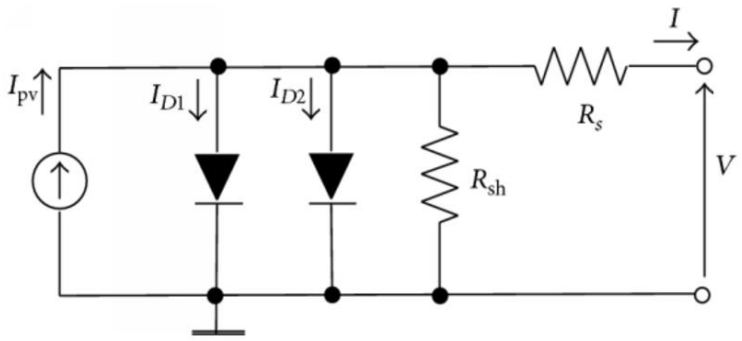

Figure 12: Two-diode solar cell's equivalent circuit.

where **R_S** is a series resistance and **R_{SH}** is a shunt resistance. These two diodes performs conductive mechanism inside the p-n junction. The equation is [1]:

$$I = I_{PV} - I_D - I_{R_{SH}} = I_{PV} - I_{D1}\{\exp[\frac{e(V+R_S I)}{\eta_1 kT}]-1\} - I_{D2}\{\exp[\frac{e(V+R_S I)}{\eta_2 kT}]-1\} - \frac{V+R_S I}{R_{SH}} \tag{6}$$

Here is the equivalent circuit of a full single-diode with series and parallel "shunt" resistances:

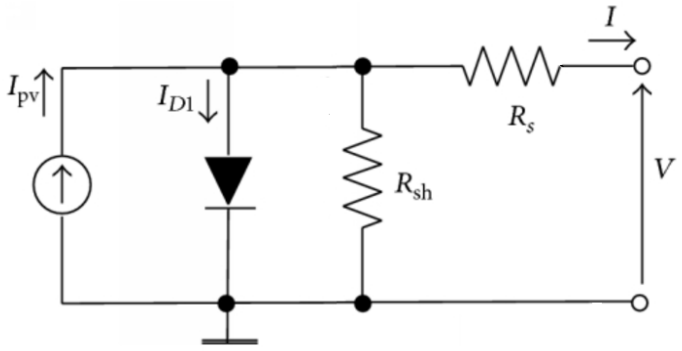

Figure 13: A full single-diode's equivalent circuit.

Here is the equation to describe a single-diode model [3] (Fig.):

$$I = A_i J_{PV} - AJ_0[\exp(q\frac{V + R_S I}{\eta kT}) - 1] - \frac{V + R_S I}{R_{sh}} \quad (7)$$

We can make a simplification of the above equivalent circuit:

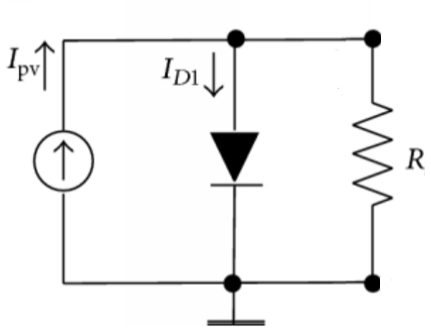

Figure 14: Simplified equivalent circuit of single diode.

moreover, equation will be [1]:

$$I = I_{PV} - I_D = I_{PV} - I_S(e^{\frac{eV}{\eta kT}} - 1) = I_{PV} - I_S(e^{\frac{eV}{V_T}} - 1) \quad (8)$$

where (6, 7, 8):

A is a total area of a sell

A_i is an illuminated area of a sell

η is a diode quality factor (close to 1)

k is a Boltzmann's constant ($1.38*10^{-23}$ J/K)

T is an absolute temperature (in K)

I is a current

I_{PV} is a photocurrent

I_D is a diode current

V is a terminal voltage

J_{PV} is a density

e is an elementary charge ($1.602*10^{-19}$ C)

I_{D1} is a diffusion current

I_{D2} is a generation-recombination current

3.4. Model of dynamic PV cells

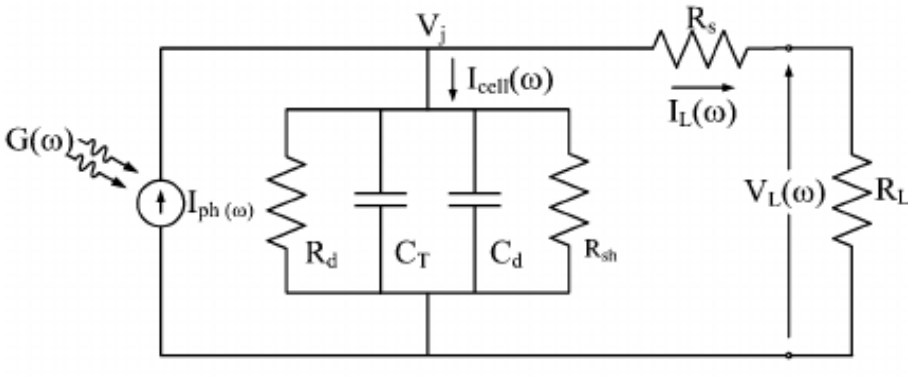

Figure 15: AC equivalent circuit of a solar cell.

Modeling the dynamic AC circuit of modules gives us important knowledge to understand when there is frequency-dependent weakening through the PV strings. We need to take into account, that dynamic modeling of frequency response of PV modules must include different temperatures, currents, voltages and irradiances.

where:

I_{PV} is a current of the module

R_{SH} is a shunt resistance

R_S is a series resistance

R_D is a dynamic resistance of the diode

C_D is a diffusion capacitance

C_T is a transition capacitance

R_L is a resistor load

$V_L(\omega)$ is a dynamic voltage

G (ω) is an irradiance

$I_{cell}(\omega)$ is a current of the cell

ω is a signal frequency

AC models are used to describe optical detectors, calculate charge densities and determine layers of the cell and to discover capacitances and resistances change with varying cell inputs like illumination or temperature.

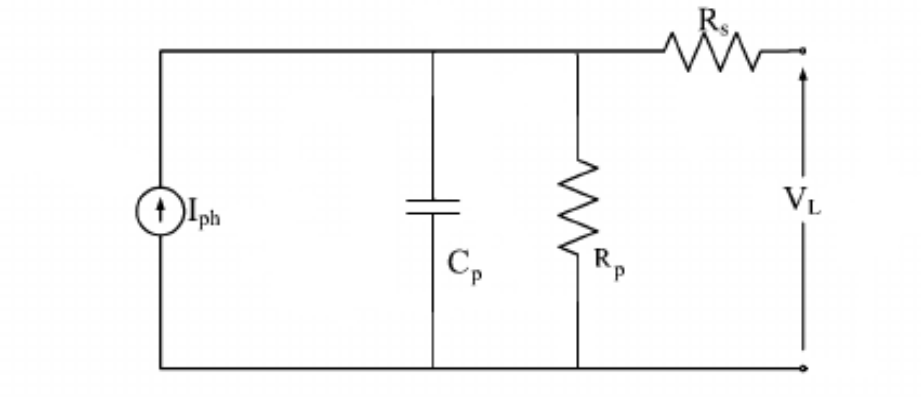

Figure 16: Simplified AC equivalent circuit of a solar cell.

where:

C_p is a combined capacitance

R_p is a resistance connected in parallel

R_s is a resistance connected in series

For calculation values of capacitance and resistance, we use impedance spectroscopy. The values of a resistor are calculated by dynamic impedance loci: **R_s** is the high frequency intercept and **R_s+ R_p** are the minimum frequency intercept. In addition, we can determine **C_p** from the measured reactance.

Complex impedance can be calculated by this formula: [6]

$$Z_{PV} = [R_s + \frac{R_p}{(\omega R_p C_p)^2 + 1}] - j[\frac{\omega R_p^2 C_p}{(\omega R_p C_p)^2 + 1}] \quad (9)$$

3.5. Shunt resistors and their effect of failures on the I-V curve.

The shunt resistance shows us a shunt track for the flow of current, which is bypass the active solar cell. The fill factor of the module alter by shunts of single solar cell. In additional, the shunt resistance influences short-circuit current and open-circuit voltage. If our shunt path shows us higher leakage current, it means that the shunt resistance is low. [12]

We can detect failures of PV module using I-V curve, which depends on the available data. In case of I-V curve without any information on the specific electrical values, we can determine:

- I_{SC} current

- V_{OC} voltage

- Fill Factor

- The shape of the I-V curve reveals two defects: non-active cell parts due to cell cracking or other reasons and short-circuit of a bypass diode.

If we know all electrical parameters, the comparison of the calculated results makes failures and technical problems easy to indicate. The third case, if we have a last I-V curve of the same PV module, which was measured by the same equipment and under the same conditions, we can evaluate the I-V curve for degradation effects and failures. [12]

On the figure below, we can see failures detectable by the I-V curve. It could be divided into the following categories:

Picture number 1: A lower I_{SC} than expected caused by the loss of transparency of the encapsulation. These effects on the I-V curve are like a reduction of the irradiance and the shape of the curve changes differently if the effects are heterogeneous or homogenous.

Picture number 2: A lower V_{OC} than expected caused by failed cell interconnections, short circuits from cell to cell or a failure of the bypass diode.

Picture number 3: The slope near V_{OC} is lower indicating an increase of the series resistance in the PV module by the increase of corrosion in junction box and interconnection resistance.

Picture number 4: The I-V curve near I_{SC} is sloped. It means that the shunt resistance decreased due to shunt paths in the PV cells.

Picture number 5: In this case, it is very often caused degradation of antireflective layer or PID effect.

Picture number 6: The I-V curve has steps. The reasons are damaged cells or a defect in the bypass diode. [12]

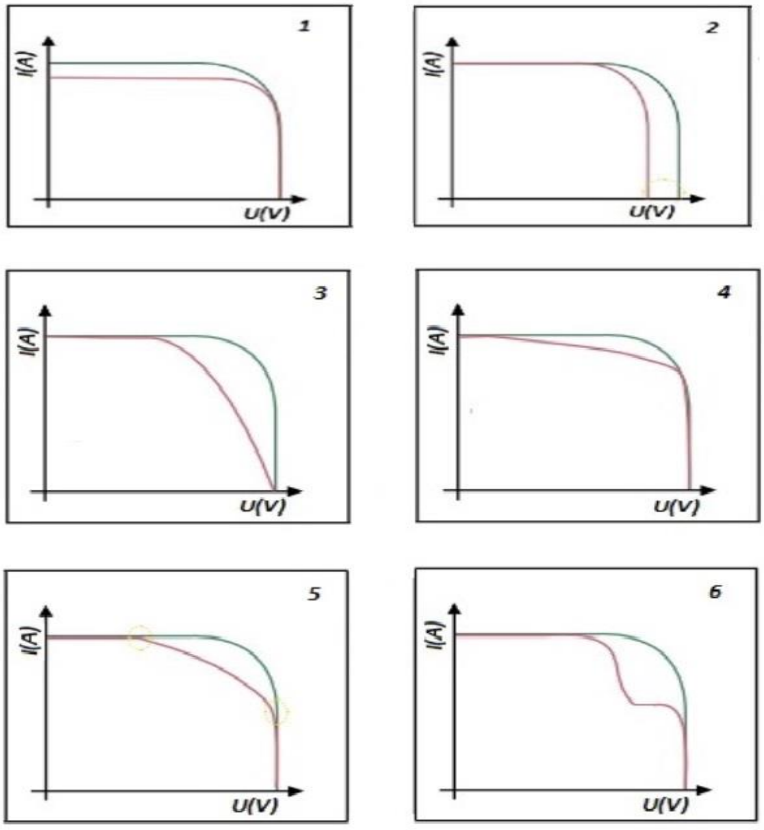

The figure 17: PV modules failures detectable by the I-V curve.

4. Methods of measurement

4.1. Impedance Spectroscopy

Impedance spectroscopy (IS) helps in understanding analysis of the experimental results. Scientists, analytics, investigators and their fundamental mechanisms describe solar cell's operations. IS presents method of electrochemical learning, which is usually investigates charge transfer between a solid conductor and an electrolyte. Additionally, the electrolyte can provide a huge amount of conductivity in the liquid phase because of salt. IS can determine the energy levels of carrier traps of solar cells in solid state. [5] We connect IS to the system by electrical contacts.

$$Z(\omega) = \frac{V(\omega)}{I(\omega)} \tag{10}$$

where: Z (ω) – Impedance spectroscopy, V (ω) – AC voltage, I (ω) – AC current.

During the measurement of IS, the whole system is in fixed steady state, and the Z (ω) is measured obtaining the frequency $f = \frac{\omega}{2\pi}$ from mHz to 10 MHz's. By these results, we can discover dynamic properties of the solar cell. Usage of IS technique is shown on the simplified figure below:

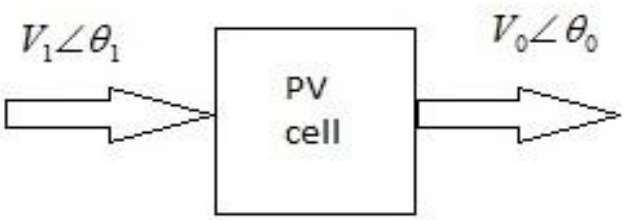

Figure 18: IS representation.

Impedance spectroscopy is very effective to characterize the solar cells. To realize these characteristics, it use measurement and analysis of all or some impedance related functions. The complex impedance Z (ω) = R (ω) + jX (ω) is obtained in a huge range of frequency, where R (ω) is the real part and jX (ω) is the imaginary part. A sinusoidal voltage in different frequencies is connected to the system under the phase shift and under the test. By these manipulations, we can measure the amplitude of the voltage and current. [6]

The dynamic impedance and their complex plane plots can observe the quality of the cell. Comparison of two PV cells are given on the figure below, one of good quality and the second one is bad quality. In the fig.19 we use the static characteristics and in the fig.20 the impedance characteristics. Due to high fill factor, good quality PV cells have rectangular shape and because of low fill factor, bad quality PV cells have triangular shape.

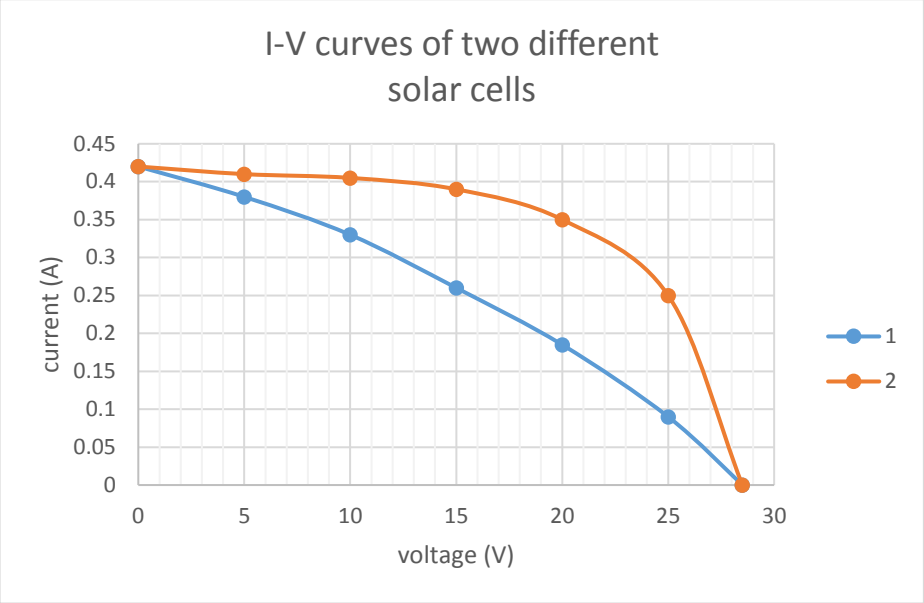

Figure 19: Comparison of two solar cells according static characteristics.

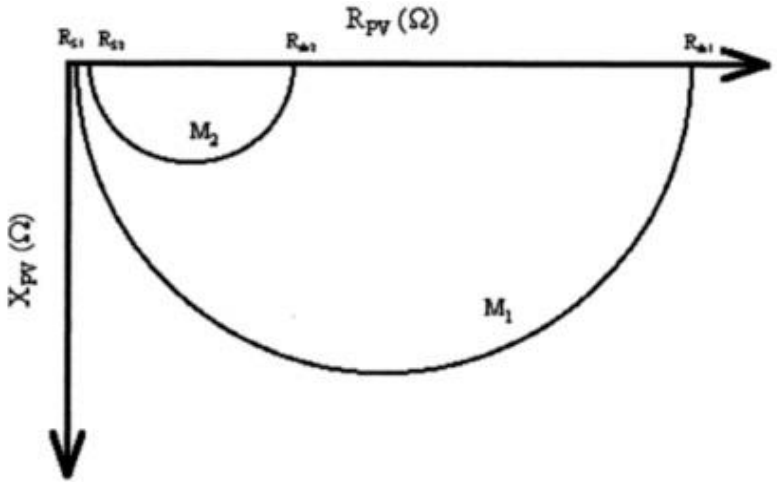

Figure 20: Comparison of two solar cells according impedance characteristics. [6]

In addition, in scanning process of the frequency, it is very important to calculate the IS parameters at various conditions of steady state. We use it for relation between the measurement and a physical model. [5] At each steady state, the impedance Z (ω) value is related to a model in the frequency domain, which we can present as an equivalent circuit. Measurement takes a long time, but finally, we get very necessary information and values to observe the dynamic properties of the system.

4.1.1. Equivalent circuits for different RC combination

Most of IS measurements are performed by equivalent circuits. These circuits are assembled by connecting RLC and other elements by wires, which are shows low resistance paths in the system.

R_1C_1 in series combination [5]:

Impedance: $Z(\omega) = R_1 + \frac{1}{i\omega C_1}$ (11)

Complex capacitance: $C^*(\omega) = \frac{C_1}{1 + i\omega\tau_1}$ (12)

Relaxation time: $\tau = R_1 C_1$ (13)

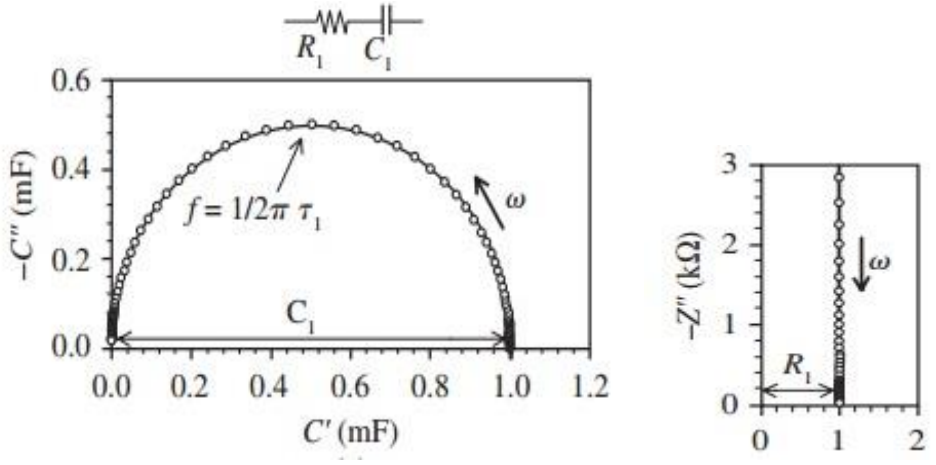

(1) (2)

Figure 21: Equivalent circuit of the impedance. R1 = 1 kΩ, C1 = 1 mF, τ1 = 1 s. [5]

From the fig.21 (1), we can see the plot of the complex capacitance C*(ω). It shows an arc from the DC value C*(0) = C_1 to the high value of the frequency. The impedance is shown in the complex plane in fig.21 (2) as a vertical line.

R_1C_1 in parallel with series R_2 [5]:

Impedance: $Z(\omega) = R_2 + Y_1 = R_2 + \frac{R_1}{1 + i\omega\tau_1}$ (14)

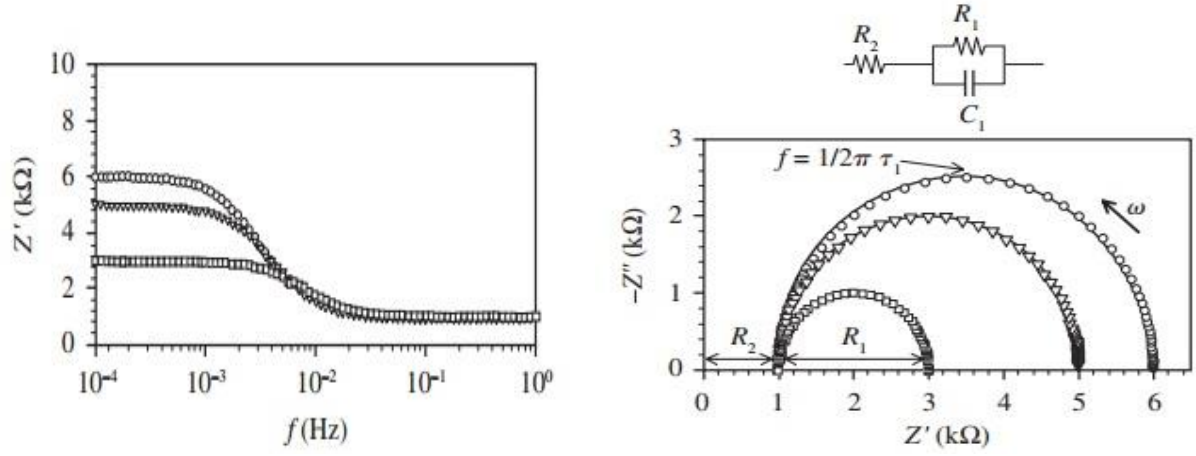

(1) (2)

Figure 22: Equivalent circuit of the impedance. R1 = 5, 4, 2 kΩ, C1 = 10 mF, τ1 = 50, 40, 20 s, R2 = 1 KΩ. [5]

From the fig.22 (1), we can see the transition of the resistance from the low frequency to the high frequency R_2. From the fig.22 (2), we can see the complex impedance plot. Using the series resistance R_2, the parallel RC forms shifted positively along the real axis. We have some changes in the characteristic time because of three plots are corresponded to variation of the parallel resistance. [5]

R, RL, C in parallel combination [5]:

Total admittance: $Y(\omega) = \frac{1}{R_1} + \frac{1}{R_3 - i\omega L_3} + i\omega C_1$ (15)

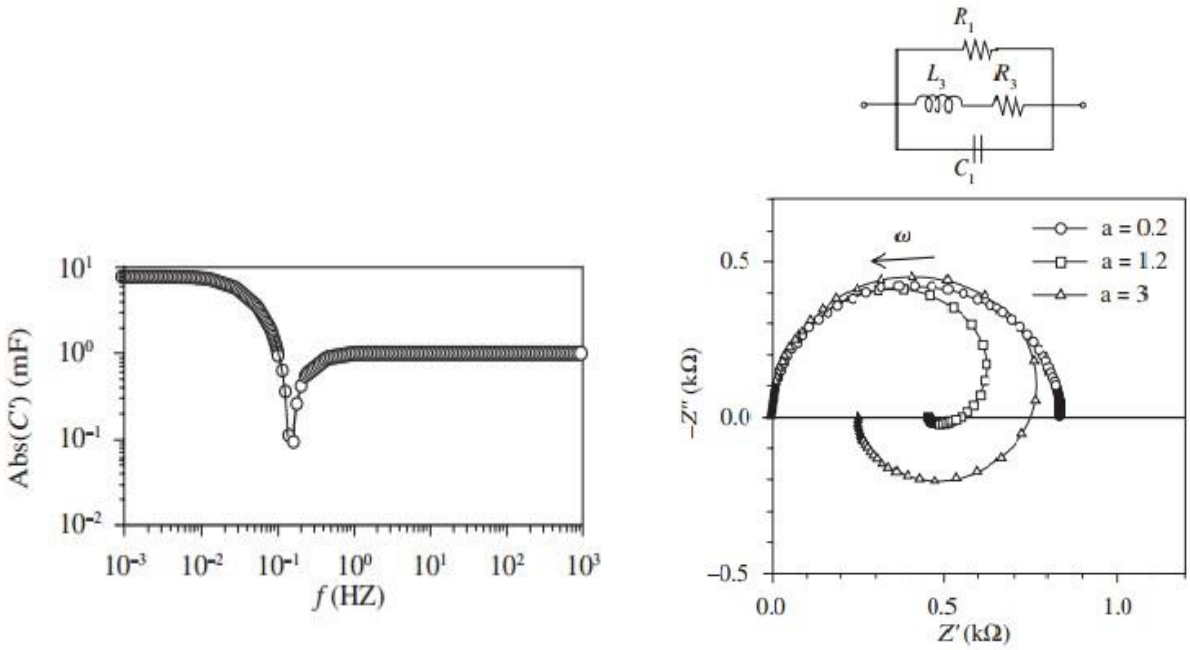

(1) (2)

Figure 23: Equivalent circuit of the impedance. R1 = 1 kΩ, C1 = 1 mF, L3 = 1 kH, R3 = R1/a. [5]

From the fig.23 (1), we can see graphical representation of capacitance and frequency. The inductor L presents as the negative contribution. From the fig.23 (2), we can see the spectra with a positive and negative low frequency capacitance. [5]

Two series RC in parallel:

Impedance: $Z(\omega) = R_1 + \frac{1}{j\omega C_1} \| R_2 + \frac{1}{j\omega C_2} = \frac{j\omega(\tau_1 + \tau_2) + 1 - \tau_1\tau_2\omega^2}{j\omega(C_1 + C_2) - \omega^2(\tau_1 C_2 + \tau_2 C_1)}$ (16)

Fig.24 (2) performs the blocking response at low frequencies. Fig.24 (1) performs several relaxations presented by two RC circuits in parallel combination. [5]

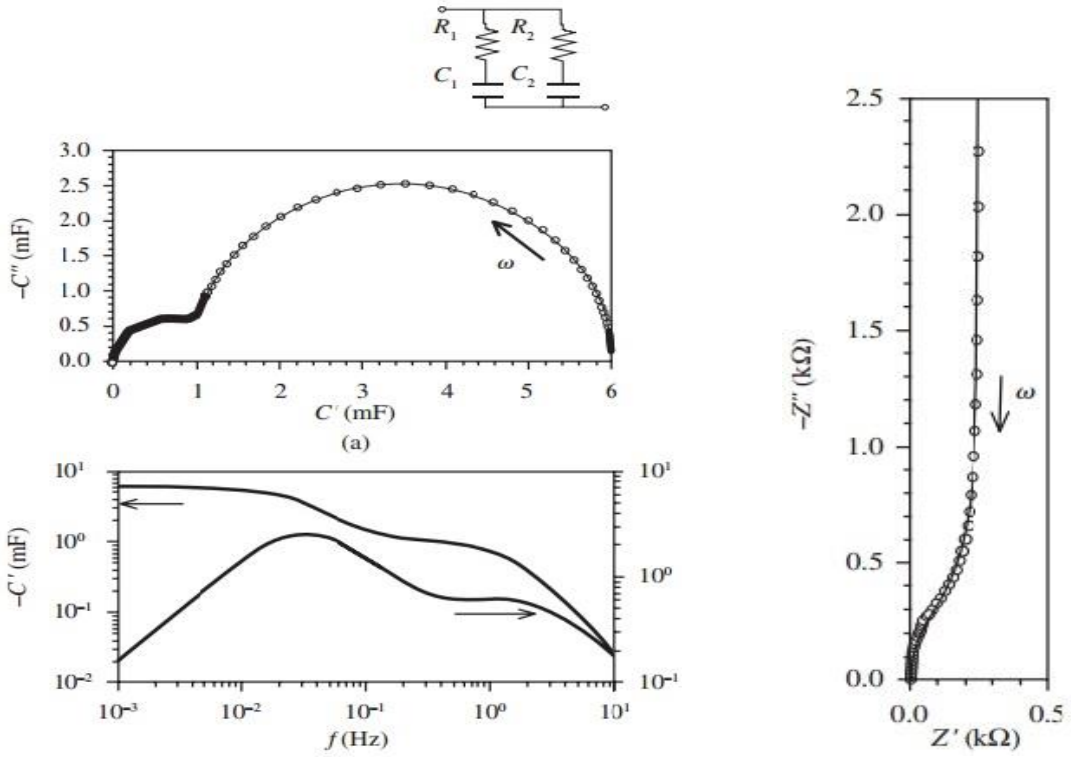

(1) (2)

Figure 24: Equivalent circuit of the impedance. R1 = 1 kΩ, C1 = 5 mF, R2 = 0.1 kΩ, C2 = 1 mF, τ1 = 5 s, τ2 = 0.1 s. [5]

4.2. Flash testers

In solar measurement, we have been used flash testers at last 30-40 years. The main advantages of these testers over continuous illumination testers are that flash testers provide high light intensity with good uniformity over large areas and the cell has no overheating because of short pulse of light. There exist two types of flash testers: the single-flash and multi-flash. Nowadays, the single one is the most frequently used system. These systems create a pulse of light that has a plateau of light intensity, which is constant, and for few milliseconds, the whole I-V curve is recorded. Because of peak power outputs have tens of kilowatts, it is very expensive and difficult to regulate flows of power. Single-flash testers and their I-V curve shaping require a high-speed electronic load for the cell and there can be some transient errors. [7]

Multi-flash testers use a huge amount of flashes to create the I-V curve. It takes only a single I-V point for each cell. In these systems are not required the regulated flash and the high-speed load. These conditions makes multi-flash testers cheaper and simpler than the single-flash testers.

Also, exist other alternative method for measuring solar cells and modules. The main advantage of such constant-voltage flash testers is that they gives more data for performance of the cell. I-

V curves gives us full information about the behavior of the cell in the case of different intensities of the light. The cell bias circuitry contains the cell at constant voltage during each flash. We use it for minimization of transient errors. It is very useful and profitable for concentrator and 1-sun cells. If we will compare this tester with a conventional one, we can definitely say that the constant-voltage system provides more information about behavior of the cell.

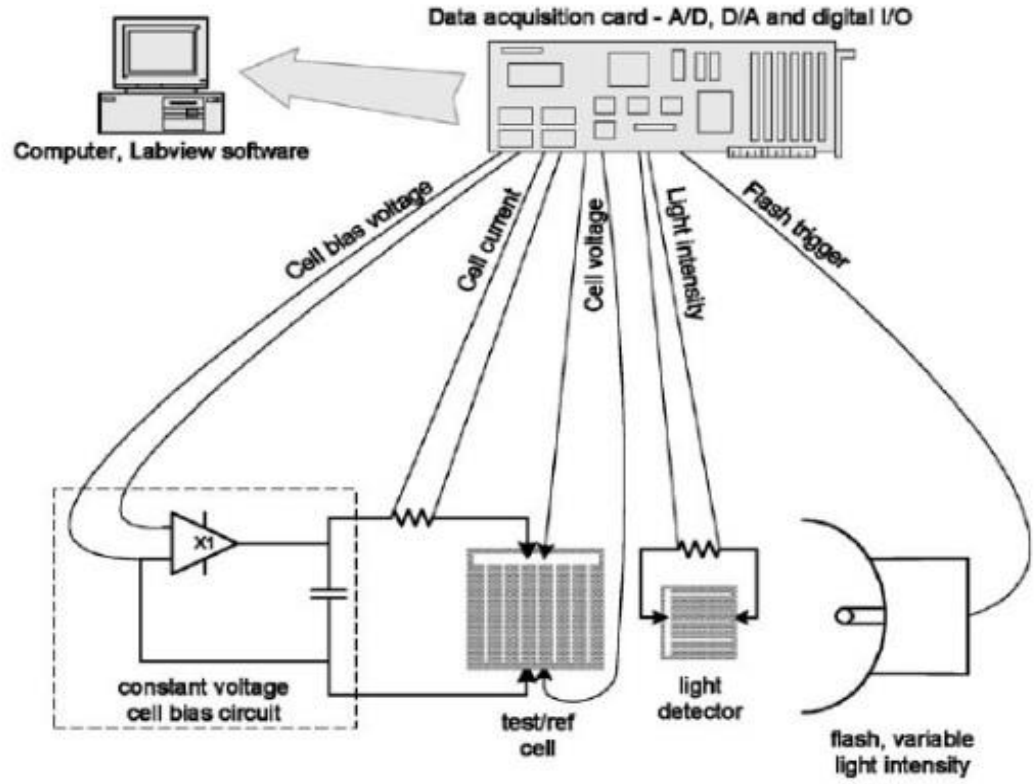

Figure 25: Flash tester's block diagram. [7]

4.2.1. Analysis of transient errors

The cell must be in quasi-steady state. We use this condition to get accurate I-V measurements. Using flash tester it is hard to exactly guarantee, so measurement errors occur because of transient effects. If the I-V curve is swept out too quickly, we can get the same problems with continuous illumination testers.

Transient errors are caused by quick changes of distribution of the charge in the cell. In the case of under illumination, there are two sources of the current that can rebuilt charge current produced by the light source and external circuit current. The magnitude of transient errors depends on the amount of excess charge stored in the cell. [7]

4.3. Electroluminescence

Electroluminescence is a luminescence excited by an electric field. It is the consequence of radiative recombination of holes and electrons in a semiconductor with wide enough bandwidth to allow exit of the light. Before the recombination, electrons and holes are separated – by doping the material to create a p-n junction or by high-energy electron's excitation, which are accelerated by a strong field. We use EL as a diagnostic tool for analysis of defects on PV cells and modules.

The cells emanate infrared light and the wavelength range is from 1000nm to 1200nm. We can find out cracks and other damages because of intensity reflects the amount of minority carriers in base layers. A silicon charged-coupled device (CCD) camera is an electrical device that is used to produce images of objects, store information and transfer electrical charge. Typically, it capture an area of 1cm in less than 1s. The most important performance has a temperature, because temperature changes resulting to different intensity contrasts of EL and it can be very useful for inquires of the results. EL is a fast optical and electrical technique for increasing the output efficiency and quality of solar cells and modules by detecting the defects, which human eye cannot see.

Usually electroluminescence panels are made up of organic and inorganic materials. They are widely used in household electrical appliances and in light technic, particularly for illumination of the LCD displays. The most popular EL devices are consist of powder and thin films.

In the figure below, we can see the in-homogeneities using the EL technique for a multicrystalline silicon solar cell.

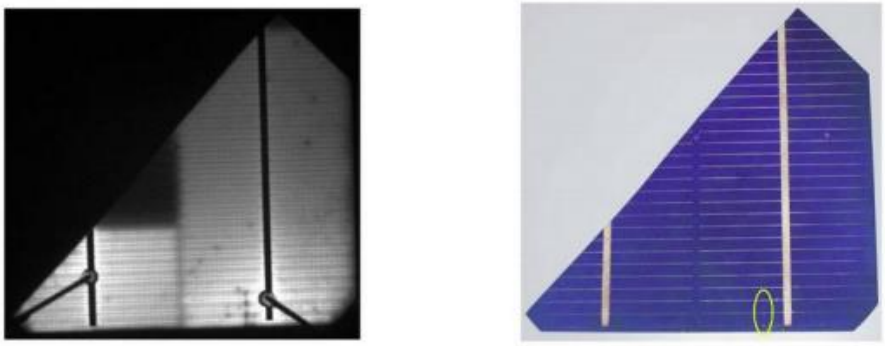

Figure 26: Multicrystalline Si solar cells with and without EL. [3]

4.3.1. Diagnostics of photo-electro-luminescence

In steady state, generation [3]: $G = \frac{d\Delta n}{dt} = -\frac{\Delta n}{\tau}$ (17)

Luminescence [3]: $\phi = (\frac{d\Delta n}{dt})_{radiation} = -\frac{\Delta n}{\tau_{radiation}} = \frac{G\tau}{\tau_{radiation}}$ (18)

Lifetime [3]: $\frac{1}{\tau} = \frac{1}{\tau_{radiative}} + \frac{1}{\tau_{recombination}} + \frac{1}{\tau_{Auger}}$ (19)

5. Practical Part

5.1. Devices for laboratory measurement

For impedance spectroscopy was used Hewlett Packard (HP) 4284A Precision LCR meter. The test frequency range is from 20Hz to 1MHz. Other important parameters are shown in the table 1 below [10]:

Line voltage	100, 120, 220 Vac ±10%б 240 Vac ±5% - 10%
Temperature	0 to 55°C
Humidity	≤ 95% R.H. at 40°C
Display	LCD dot-matrix display
Power consumption	200 VA max

Table 1: Basic parameters of HP 4284A Precision LCR meter.

Figure 27: During laboratory measurement of IS.

Device GSolar GEL-M4 was used for electroluminescence laboratory measurements. We can test the PV solar modules before and after lamination. It can detect different types of defect, for

example, cracks, material defect, low efficiency solar cell area, micro cracks etc. Usable for both monocrystalline and multicrystalline. Other important parameters are shown in the table 2 below [9]:

Module face	Down
Visual range	2000x1100mm
Power supply	220V 10A, single phase
Max. input voltage	120V
Max. input current	10A
Pixel resolution	4928x3264
Ambiance (temperature and humidity)	Tem 20-30°C Hum 40-70%

Table 2: Basic parameters of GSolar GEL-M4.

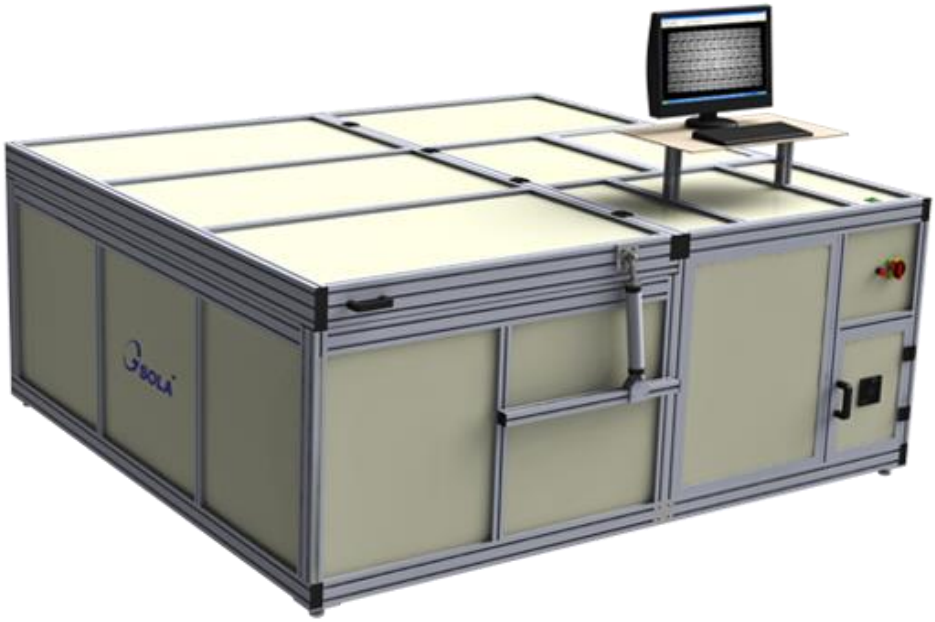

Figure 28: The EL tester [9].

For flash tester was used the Pasan SunSim 3c. For optional parts we have the black tunnel optical filters and light attenuation masks. The standard parts are [11]:

- Electronic load

- Monitor cell

- Flash generator and light box

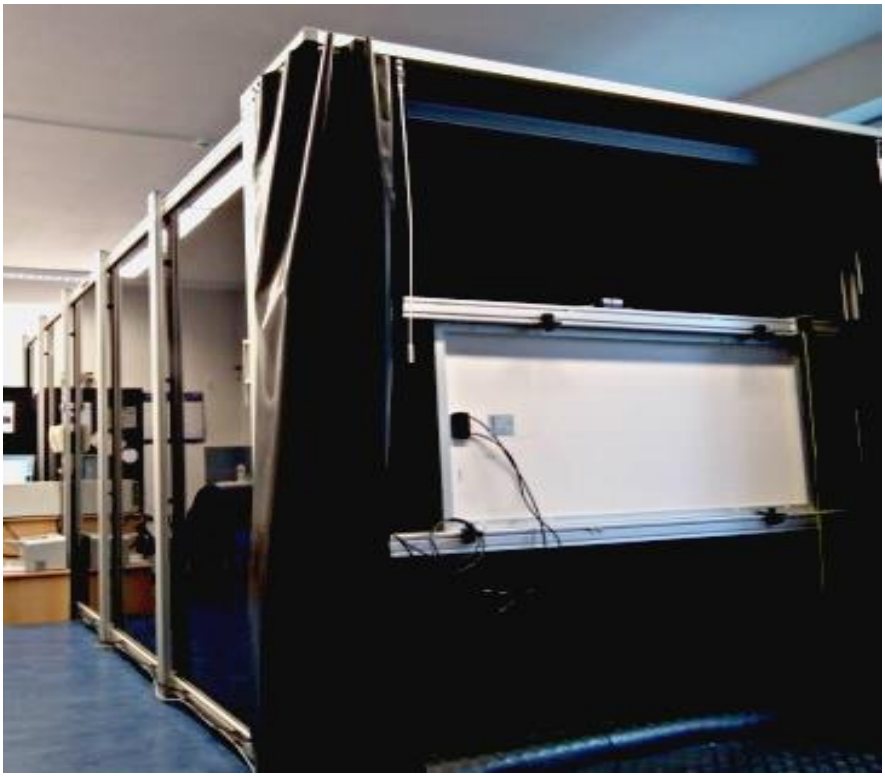

Figure 29: During laboratory measurement of Flash Tester.

5.2. Solar cells for laboratory measurement

All modules that we measured have the same characteristics.

Phono Solar. Module Type PS15 (M). The important parameters are shown in the table 3 below:

Rated Power at STC	Wp	15	W
Rater Power Voltage	Vm	2.1	V
Rated Power Current	Im	7.5	A
Open Circuit Voltage	Voc	2.71	V
Short Circuit Current	Isc	8.04	A
Nominal Operation Cell Temp	NOCT	45˚C±2˚C	
Maximum Fuse Rating		10A	
Application Class		A	
Dimension		376x376mm	

Table 3: Basic parameters of PS15 (M).

5.2.1. Summary

Three different methods are used – Impedance Spectroscopy, Electroluminescence and Flash Test. The main aim of these laboratory measurements is the process and technical description of

the diagnosis of PV cells and modules. By these measurements, we recognized that IS is very effective analysis method for describing the solar cell's operations. By this method, we can determine dynamic parameters and analyze the quality of the cell. The EL is an optical technique resulting in we find out possible cracks and damages on a cell. In the case of Flash Tester, we use a dark tunnel where a flash emits a high light intensity to record I-V curves.

5.3. Obtained results

5.3.1. Impedance spectroscopy

All values in this graph, except module number 16, are approximately the same. We measured 20 PV modules and choose 5 of them: modules 5, 6 (monocrystalline), modules 11, 12 (multicrystalline) and defective module number 16.

By measuring the dynamic parameters of these modules in a range of frequency from 20Hz to 1MHz, we plotted the real and imaginary parts on complex plane in dependence on frequency. This method is not good for multicrystalline. In additional, it is not transparent as in monocrystalline. We use the impedance spectrum of the system, which is called cole-cole plots. The cole-cole is a graphical representation of real and imaginary parts, which gives us the impedance arcs. From these arcs, we obtain the different AC parameters. (Values that were used to plot this graph can be found in annex A).

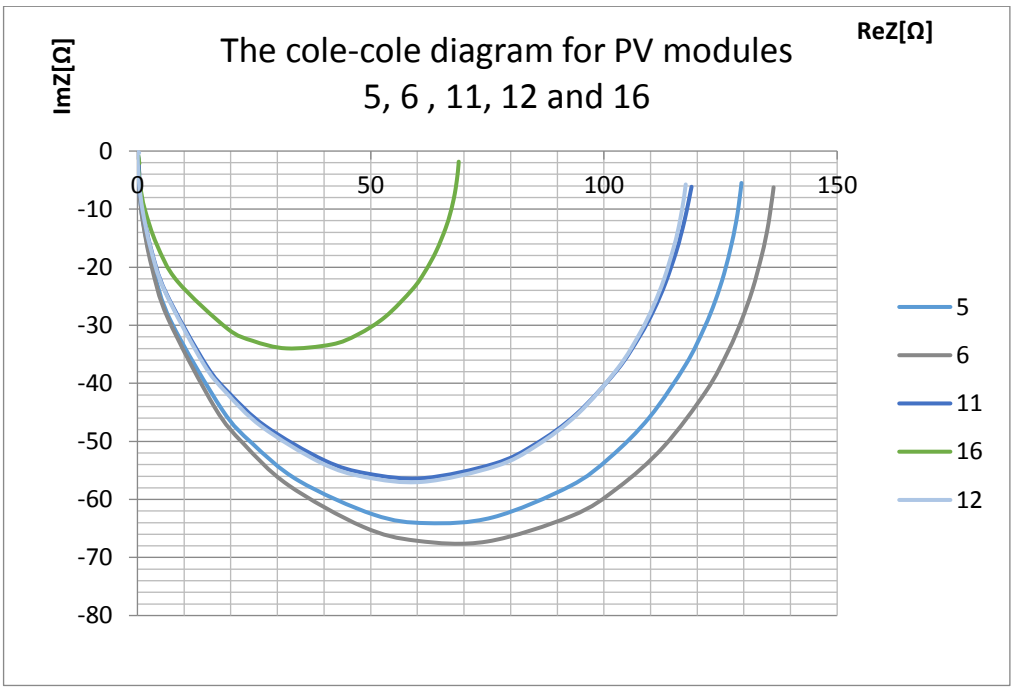
The cole-cole diagram for PV modules
5, 6 , 11, 12 and 16
ImZ[Ω]
ReZ[Ω]
0
-10
-20
-30
-40
-50
-60
-70
-80
0
50
100
150
5
6
11
16
12

Czech Technical University in Prague
Faculty of Electrical Engineering

Department of Electrotechnology

BACHELOR THESIS ASSIGNMENT

First name and family name of student: **Meiirbek Nariman**

Study programme: Electrical Engineering, Power Engineering and Management
Specialisation: Applied Electrical Engineering

Title of Bachelor Project: **Diagnosis of photovoltaic modules using alternate methods of measurement**

Guidelines:

1. Process and describe the problematics of PV modules diagnostics with focus on Impedance Spectroscopy, Electroluminescence and Flash test measurement methods and influence of paralel rezistors .
2. Apply the methods mentioned above on the set of crystalline silicon PV modules.
3. Discuss the results in terms of comparing results.

Bibliography/Sources:

[1] Gray, Jeffery L. The Physics of the Solar Cell. A. Luque a S. Hegedus. Handbook of Photovoltaic Science and Engineering. Chichester : John Wiley & Sons, Ltd., 2003, 3.
[2] CHEVNIDHYA, D., K. KIRTIKARA a C. JIVACATE Dynamic Impedance Characterization of Solar Cells and PV Modules Based on Frequency and Time Domain Analyses. Trends In Solar Energy Research. Hough, T.P. New York: Nova Science Publishers, 2006, s. 21-45. ISBN 1-59454-866-8; LCCN: 2005034740.
[3]Taylor, N. (Ed.): Guidelinesfor PV PowerMeasurement in Industry, Italy: EuropeanComission, Joint Research Centre, Institute forEnergy. 2010-04. Cite 2011. ISBN: 978-92-79-15780-6.

Bachelor Project Supervisor: **Ing. Tomáš Finsterle**

Valid until the end of the summer semester of academic year 2017/2018

Figure 30: The cole-cole plots for PV modules 5, 6, 11, 12 and 16.

Dynamic parameters of the solar cell show us the quality of the modules. In our case, module number 16 has the lowest quality, modules 11, 12 have medium quality and modules 5, 6 have the highest quality. In additional, module number 16 has the lowest FF and efficiency, modules 5, 6 have the biggest FF and the best efficiency and modules 11, 12 have medium FF and efficiency.

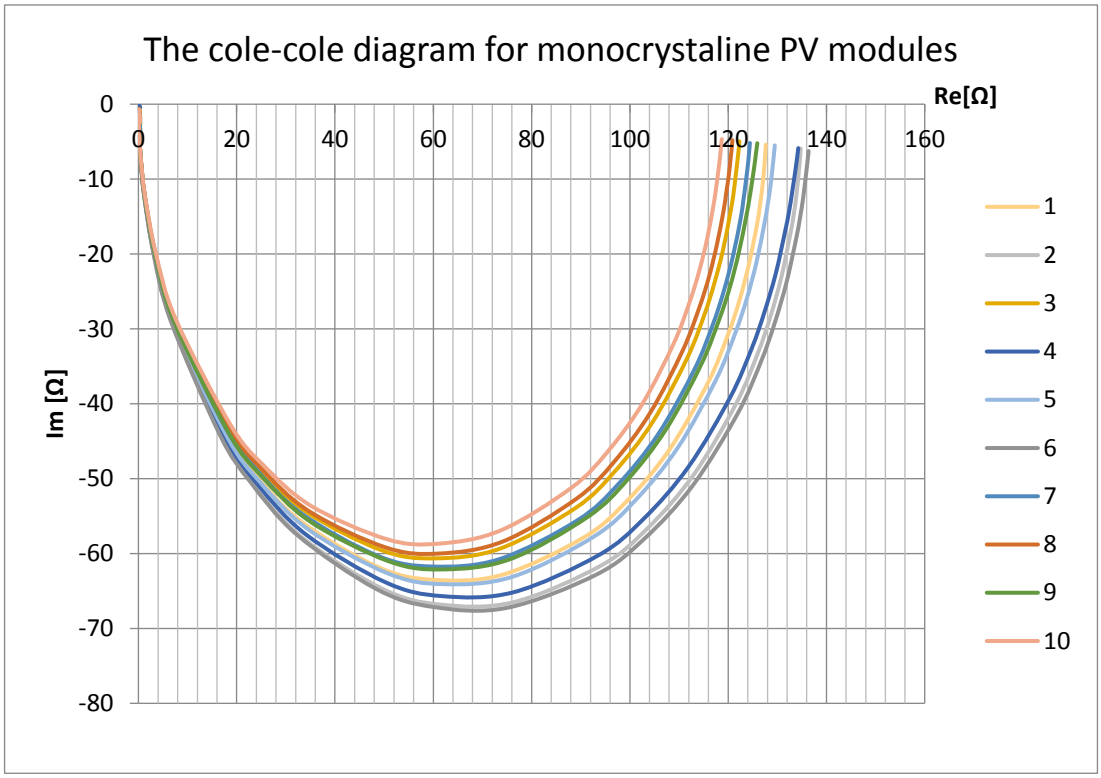

Figure 31: The cole-cole plots for all monocrystalline PV modules.

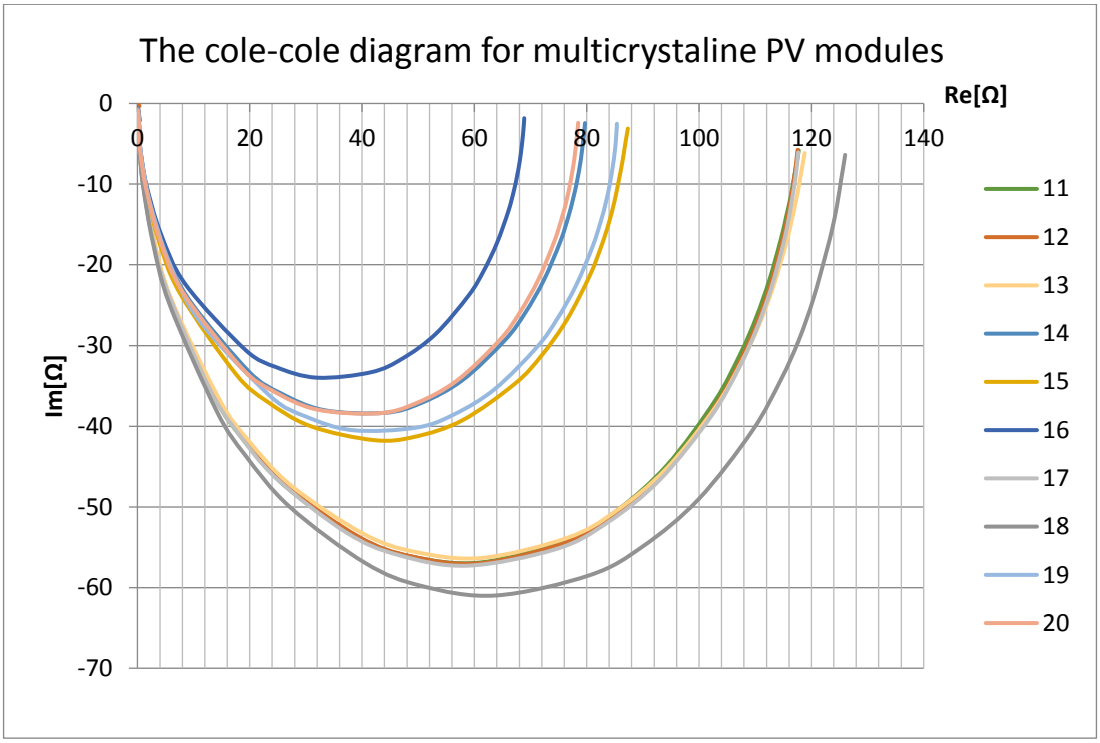

Figure 32: The cole-cole plots for all multicrystalline PV modules.

From the figures above, we can see that IS is a very good diagnostic method for monocrystalline modules. The cole-cole diagrams of monocrystalline modules are approximately the same. The cole-cole diagrams of multicrystalline modules are influenced by various characteristics at the edges of individual crystal in the use of silicon.

5.3.2. Electroluminescence

As was mentioned above, we measured 20 PV modules, but this time choose 6 of them to display the pictures from EL measurement. (Pictures of other modules can be found in annex B).

Module 5

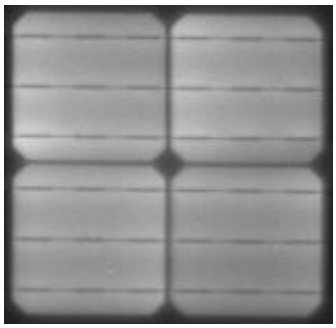

Module 6

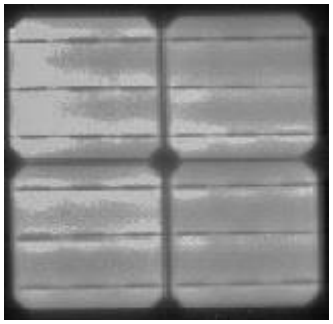

Module 11

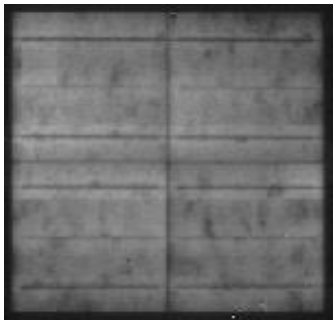

Module 12

Module 14

Module 16

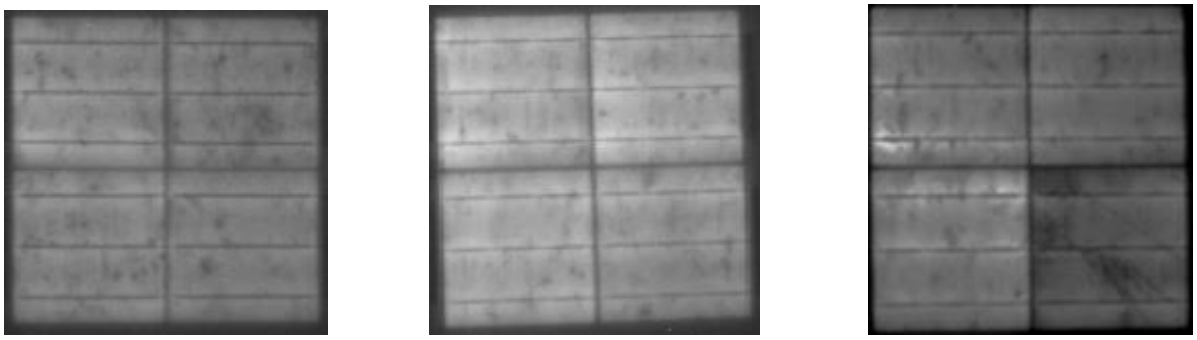

Figure 33: EL measurement results for modules 5, 6, 11, 12 and 16.

By these measured results, we can see that modules number 5, 6 without any cracks. If we will compare it with pictures for multicrystalline modules, we can see that number 11, 12, 14 have some small defects around the edges. The worst performance have module number 16. We can observe a crack on the right-down side of the module. Cracks like this decrease the efficiency and output power. To avoid problems with such defects we use this photographic optical phenomenon, which is called Electroluminescence.

5.3.3. Flash Tester

Using this method, we can compare important parameters among the modules such as efficiency, fill factor, maximum power value etc. Flash testers, also called Sun simulators, provide high light intensity with good uniformity over big areas and because of short pulse of light, the cell has no overheating.

The tables and diagrams below, show us I-V and P-V for direct 1_56R, 1_180R and 1_27K. (Other diagrams can be found in annex C).

Producer	Phonosolar
Type	PS15M
Serial number	1_56R
Designation in LPVS	
Date of the laboratory measurement	27-04-17
Actual temperature	22.2 °C
The values are converter to the temperature	25 °C
G	1.0 kW/m^2
I_{SC}	8.957 A
V_{OC}	2.524 V
η	11.08 %
FF	69.29 %
P_{max}	15.667 W
V_{Pmax}	1.903 V
I_{Pmax}	8.231 A
R_s	0.1 Ω
R_p	22.8 Ω

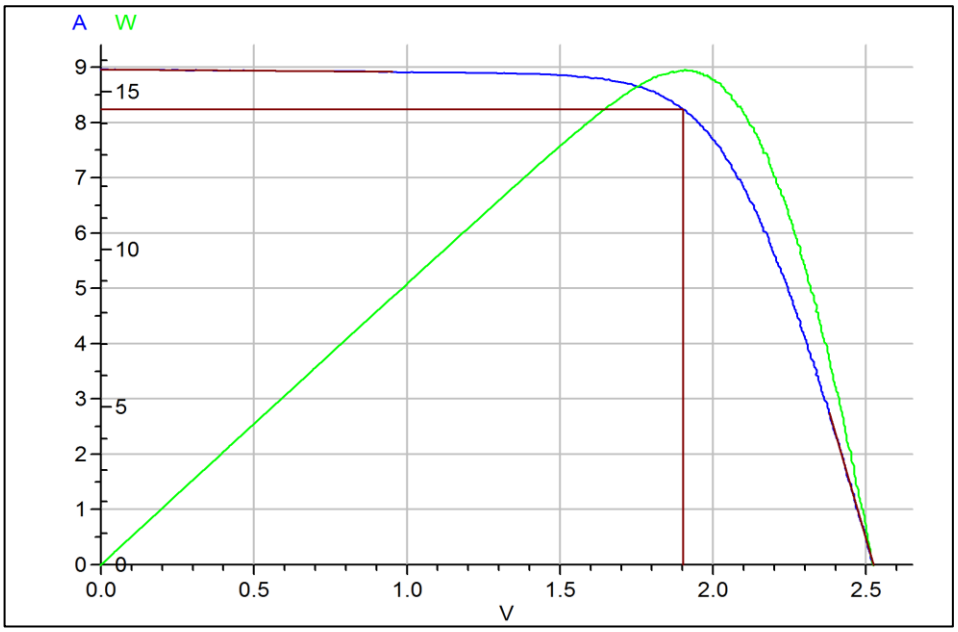

Figure 34: I-V and P-V diagrams for direct 1_56R.

Producer	Phonosolar
Type	PS15M
Serial number	1_180R
Designation in LPVS	
Date of the laboratory measurement	27-04-17
Actual temperature	22.2 °C
The values are converter to the temperature	25 °C
G	1.0 kW/m^2
I_{SC}	8.955 A
V_{OC}	2.525 V
η	11.12 %
FF	69.53 %
P_{max}	15.719 W
V_{Pmax}	1.903 V
I_{Pmax}	8.258 A
R_s	0.1 Ω
R_p	36.9 Ω

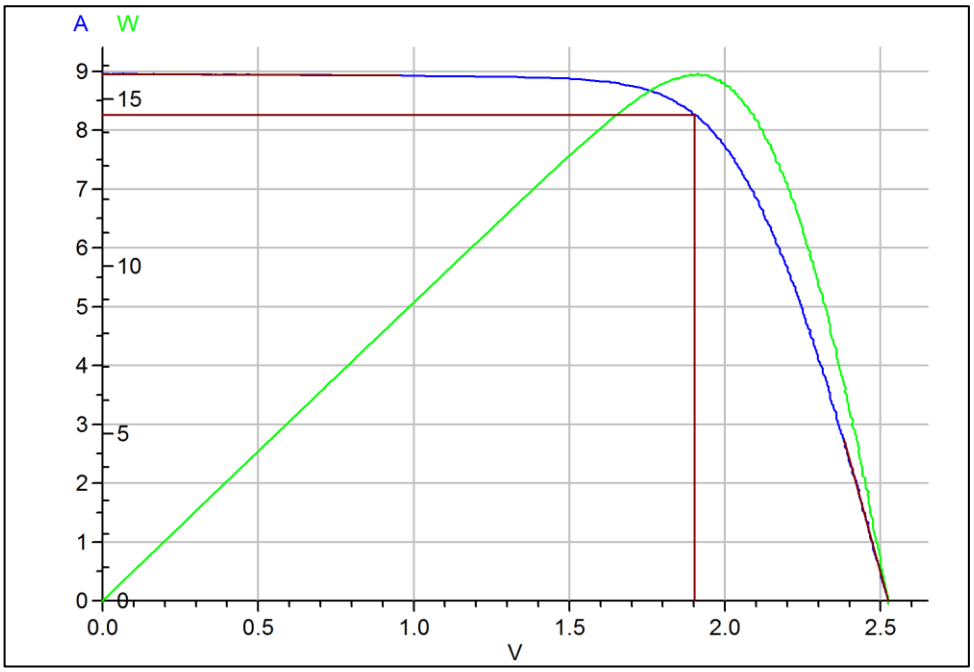

Figure 35: I-V and P-V diagrams for direct 1_180R.

Producer	Phonosolar
Type	PS15M
Serial number	1_27K
Designation in LPVS	
Date of the laboratory measurement	27-04-17
Actual temperature	22.3 °C
The values are converter to the temperature	25 °C
G	1.0 kW/m^2
I_{SC}	8.961 A
V_{OC}	2.526 V
η	11.12 %
FF	69.49 %
P_{max}	15.728 W
V_{Pmax}	1.903 V
I_{Pmax}	8.263 A
R_s	0.1 Ω
R_p	46.0 Ω

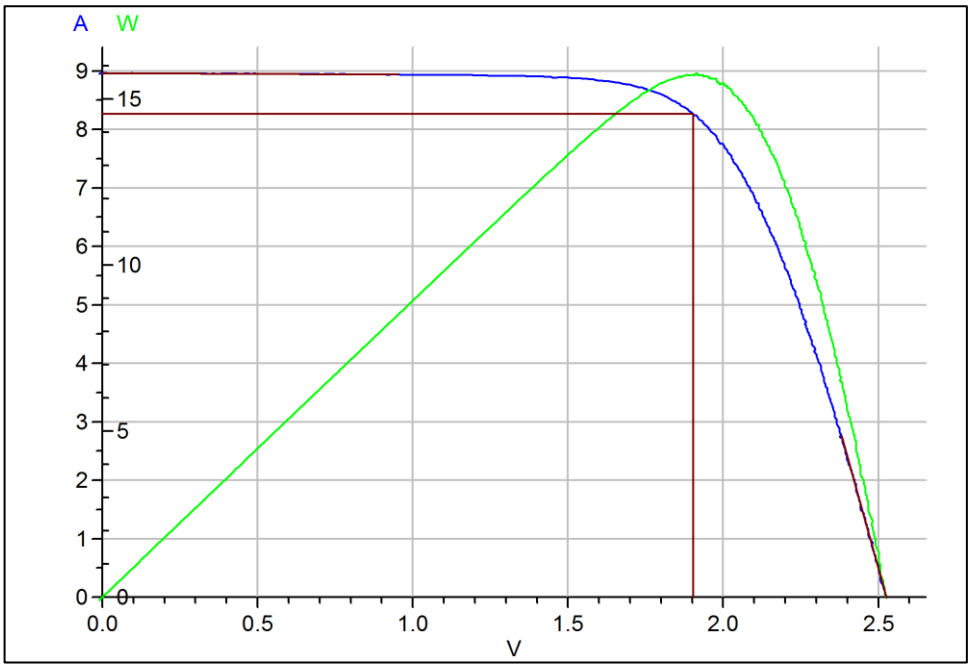

Figure 36: I-V and P-V diagrams for direct 1_27K.

The graph below show us I-V curves for the 1_56R, 1_180R and 1_27K panels with different resistors. (used values for plotting these curves can be found in annex D):

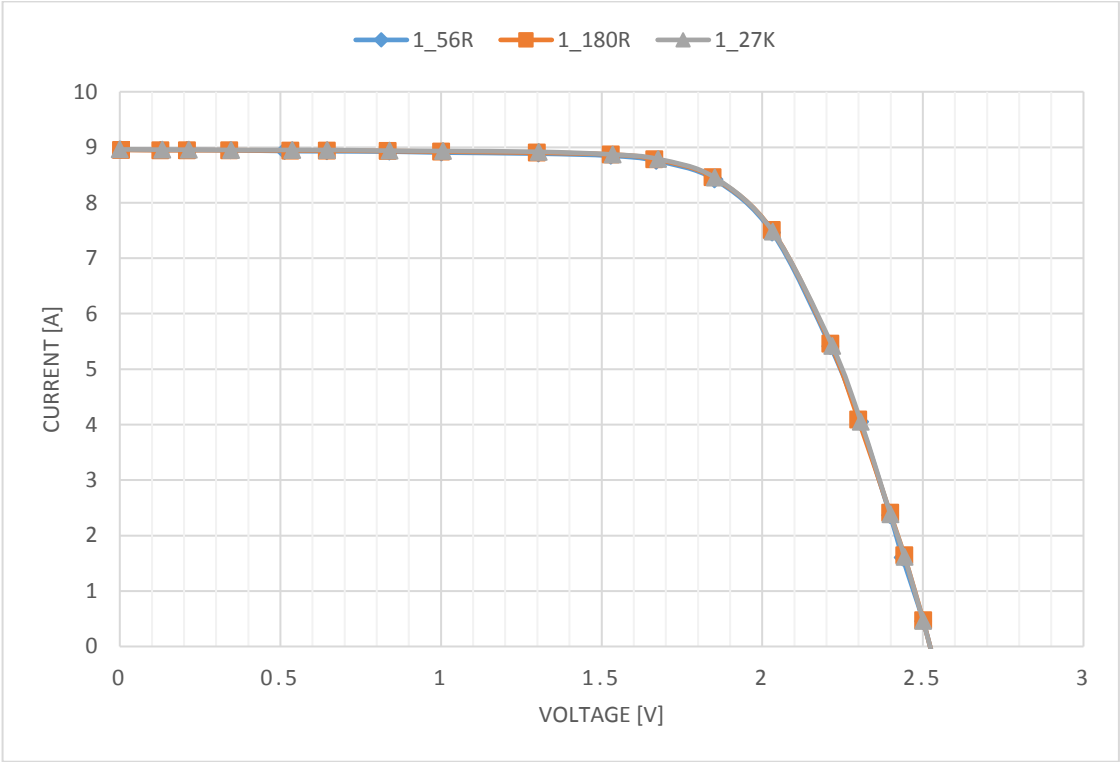

Figure 37: I-V curve for 1_56R, 1_180R and 1_27K.

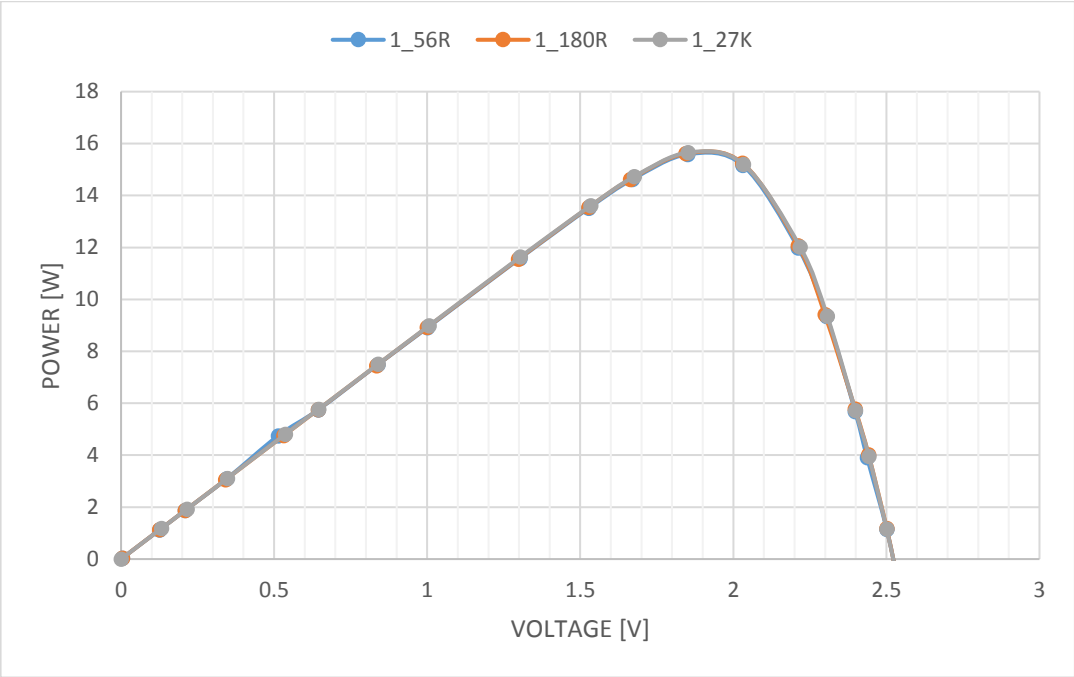

Figure 38: P-V curve for 1_56R, 1_180R and 1_27K.

By these graphs, we can say that panel with 1_27K resistor has better performance in comparison with 1_56R and 1_180R. In additional, 1_27K has bigger output and efficiency. Difference between these curves is hardly appreciable.

We can summarize the basic parameters measured for 1_56R, 1_180R and 1_27K panels:

	1_56R	**1_180R**	**1_27K**
P_{max}[w]	15.667	15.719	15.728
FF[%]	69.29	69.53	69.49
η[%]	11.08	11.12	11.12
I_{SC}[A]	8.957	8.955	8.961
V_{OC}[V]	2.524	2.525	2.526
R_s[Ω]	0.1	0.1	0.1
R_p[Ω]	22.8	36.9	46.0

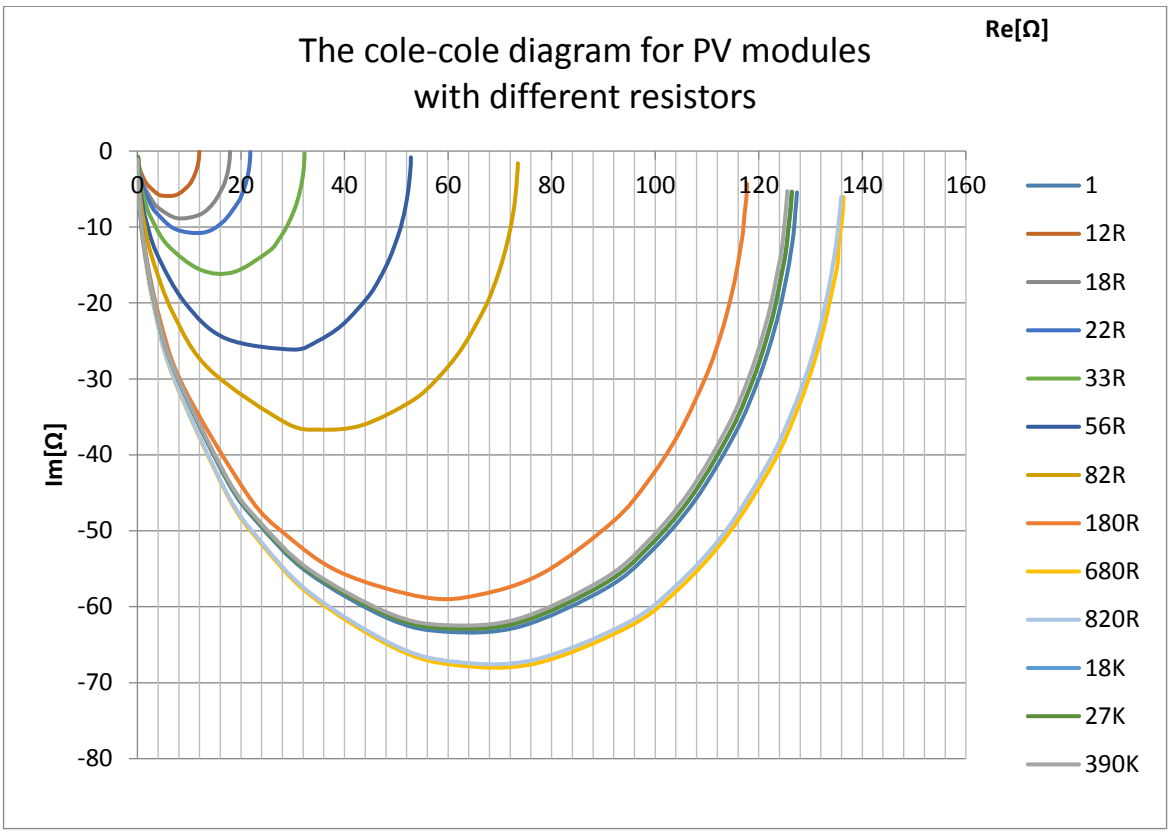

Figure 39: The cole-cole plots for all PV modules with different resistors.

1(without resistor)	**12R**	**18R**	**22R**	**33R**	**56R**	**82R**
58.7 Ω	9.4 Ω	13.9 Ω	16.3 Ω	19.1 Ω	22.8 Ω	29.5 Ω
180R	**680R**	**820R**	**18K**	**27K**	**390K**	
36.9 Ω	45.5 Ω	46.1 Ω	55.5 Ω	46 Ω	46.8 Ω	

Table 4: Comparison of shunt resistances.

From the table above, we can see that PV module without any resistor and with resistor 18K has the biggest value of shunt resistance. However, if we observe the fig.39, we can obtain correct performances on the low level, from 12R to 180R. On the high level, it makes some mistakes and we can see that the best performances have modules with resistors 680R and 820R. The worst results has the module with resistor 12R.

6 Conclusion

The problem of developing non-traditional and renewable energy sources is becoming more urgent. Non-traditional renewable energy sources include solar, wind, geothermal, biomass and energy of the World Ocean. Recently, interest in the problem of using solar energy has sharply increased. The reserves of solar energy are almost inexhaustible, because astronomers have calculated that the Sun will "burn" in the next million years. Taking into account the results of existing forecasts for the depletion of oil, natural gas and other traditional energy resources in the end of the next century, as well as reduction of coal consumption (which is estimated to be 300 years) due to harmful emissions into the atmosphere, solar and hydroelectric sources will prevail over other sources for a long time.

In this bachelor thesis, I described diagnostic of PV modules using alternate methods of measurement. I focused on PV modules construction and type of crystalline Si. For these measurements were used Impedance Spectroscopy, Electroluminescence and Flash Tester. During the work, we recognized that IS is very effective analysis method for describing the solar cell's operations. By this method, we can determine dynamic parameters and analyze the quality of the cell. The range of the measurement of all or some impedance related functions from 20Hz to 1MHz. This large range gives us important information in detail comparing with other methods. The main objective of such methods is improvement of the parameters, so we can get more efficiency.

For detection possible cracks or damages on a cell, we use Electroluminescence. A silicon charged-coupled device (CCD) camera is used to store information, transfer electrical charge and create images of the objects. By this method, we found out module 16, which was damaged on the downright side. However, this defection has no impact on the operation of the module. The EL is a very useful technique, because it is a fast optical detection for increasing the output efficiency and quality of solar cells, which human eyes cannot see.

The last one is a Flash Tester. In this method, we measure PV modules in a dark tunnel where a flash emits intensity of a high light. It takes a few milliseconds, and in this time, the I-V curve is recorded using computer with a software and the important parameters such as open-circuit voltage, short-circuit current, fill factor, maximum power point, efficiency, series and shunt resistors.

During the Flash Test measurement, we recognized that monocrystalline PV modules have better results than the multicrystalline. However, difference between the curves of panels hardly appreciable. From the fig.37 and fig.38, we cannot see that panel with resistor 27K has the biggest values of output and efficiency but in fig.39 of the cole-cole diagrams of PV modules, we can see that module 27K is the best and module 56R is the worst.

The IS measurement performed more apparently differences between defective and good PV modules. Perhaps this type of measurement is more effective and sensitive to defining of some type of defects than Flash Test.

7 REFERENCES:

[1] Gray, Jeffery L. The Physics of the Solar Cell. A. Luque a S. Hegedus. Handbook of Photovoltaic Science and Engineering. Chichester : John Wiley & Sons, Ltd., 2003, 3.

[2] Solar Electricity - Photovoltaic Systems and Components, Grid-Connected Solar Electric Systems, Off-Grid (Stand Alone) Solar Electric Systems, PV Modules, PV Inverters, PV Chargers, PV Battery, PV Mounting, Small Solar Electric Devices. Solar Direct [online]. Copyright © 1986 [cit. 14.04.2017]. Available at: http://www.solardirect.com/pv/systems/systems.htm

[3] Holovský, Jakub. SOLAR ENERGY APPLICATION SYSTEMS [online]. Available at: http://ocw.cvut.cz/moodle/course/view.php?id=302

[4] PVeducation. *PVEducation*[online]. Available at: http://pveducation.org/

[5] GDFO [online]. Copyright © [cit. 09.04.2017]. Available at: http://www.elp.uji.es/recursos/paper107.pdf

[6] CHENVIDHYA, D., K. KIRTIKARA a C. JIVACATE Dynamic Impedance Characterization of Solar Cells and PV Modules Based on Frequency and Time Domain Analyses. Trends In Solar Energy Research. Hough, T.P. New York: Nova Science Publishers, 2006, s. 21-45. ISBN 1-59454-866-8; LCCN: 2005034740.

[7] ARC Centre of Excellence for Solar Energy Systems - ANU [online]. Copyright © [cit. 13.04.2017]. Available at: http://solararc.anu.edu.au/pubs/flash_tester_SEMSC.pdf

[8] EPIA. GLOBAL MARKET OUTLOOK: For Photovoltaics 2014-2018 [online]. 2015 [cit. 2015-05-20]. ISBN 9789082228403. Available at: http://www.epia.org/news/publications/

[9] GSOLAER POWER CO.,LTD | Products. [online]. Copyright © 2011 [cit. 25.04.2017]. Available at: http://www.gsola.cn/page_en/products.html

[10] 4284A Precision LCR Meter, 20 Hz to 1 MHz [Obsolete] | Keysight (formerly Agilent's Electronic Measurement). [online]. Copyright © Keysight Technologies 2000 [cit. 27.04.2017]. Available at: http://www.keysight.com/en/pd-1000000874%3Aepsg%3Apro-pn-4284A/precision-lcr-meter-20-hz-to-1-mhz?nid=-32776.536880951&cc=CZ&lc=eng

[11] Liquidation Auction - Equipment Auctions| HGP Industrial Auction [online]. Available at: http://www.hgpauction.com/auctiondata/20110197/Pasan%20SunSim%203c%20Tester%20System.pdf

[12] KÖNTGES, Marc, Sarah KURTZ a Corinne PACKARD. *Review of Failures of Photovoltaic Modules*. International Energy Agency, 2014. ISBN 978-3-906042-16-9.

8 ANNEXES:

1 [A] Impedance Spectroscopy measurement values

	Module 5		Module 6		Module 11	
f(Hz)	**Re (ohm)**	**Im (ohm)**	**Re (ohm)**	**Im (ohm)**	**Re (ohm)**	**Im (ohm)**
20	129,488998	-5,49555	136,376007	-6,25158	117,746002	-5,8065
25	129,300995	-6,84008	136,126999	-7,77521	117,407997	-7,21066
30	129,082993	-8,17334	135,860001	-9,29007	117,046997	-8,60148
40	128,634995	-10,8137	135,296005	-12,3593	116,360001	-11,3569
50	128,026001	-13,4947	134,602005	-15,269	115,488998	-14,0726
60	127,347	-16,0702	133,759995	-18,2141	114,598	-16,7115
80	125,765999	-21,105801	131,822006	-23,931801	112,545998	-21,807301
100	123,829002	-25,895399	129,421005	-29,327999	110,153	-26,5382
120	121,495003	-30,486601	126,668999	-34,399601	107,387001	-30,961201
150	117,517998	-36,807499	121,908997	-41,347	102,803001	-36,877701
200	109,829002	-45,789799	112,803001	-50,911499	94,322403	-44,8097
250	101,352997	-52,728001	102,977997	-58,003502	85,449501	-50,413101
300	92,659897	-57,740898	93,112297	-62,831501	76,777901	-54,014999
400	76,158798	-63,091499	74,953499	-67,249901	61,283199	-56,877701
500	62,0532	-64,0839	60,0051	-67,128998	48,874401	-56,167801
600	50,640598	-62,617001	48,281799	-64,684502	39,306	-53,7556
800	34,545898	-56,767502	32,291901	-57,504398	26,397301	-47,4841
1000	24,554899	-50,306801	22,6777	-50,348801	18,6681	-41,495499
1200	18,153601	-44,540199	16,639099	-44,236401	13,8029	-36,4543
2000	7,23526	-29,4177	6,55426	-28,841801	5,58629	-23,850401
3000	3,34532	-20,257	3,02338	-19,7731	2,64389	-16,4147
5000	1,24833	-12,3668	1,13212	-12,0486	1,02629	-10,0477
8000	0,511939	-7,78067	0,469538	-7,58308	0,440256	-6,34611
10000	0,341344	-6,23774	0,31593	-6,08432	0,300557	-5,09967
15000	0,172785	-4,17443	0,164056	-4,08531	0,158973	-3,43344
20000	0,114821	-3,14341	0,1118	-3,09111	0,108712	-2,60341
30000	0,07588	-2,11893	0,076264	-2,11133	0,073966	-1,78564
40000	0,064768	-1,6142	0,066143	-1,63687	0,064321	-1,39108
50000	0,062172	-1,31782	0,063405	-1,36503	0,062284	-1,16684
60000	0,062899	-1,12614	0,064069	-1,19467	0,063481	-1,02831
80000	0,068633	-0,900901	0,069314	-1,00756	0,069968	-0,880666
100000	0,076402	-0,781396	0,076919	-0,923441	0,078437	-0,820257
120000	0,084823	-0,715543	0,085216	-0,891239	0,087451	-0,804017
150000	0,097322	-0,670794	0,098302	-0,896022	0,101016	-0,824463
200000	0,117818	-0,669738	0,120109	-0,976002	0,122919	-0,919691
250000	0,13766	-0,713575	0,141418	-1,10042	0,14385	-1,0526
300000	0,156254	-0,781028	0,161632	-1,2478	0,16366	-1,20524
400000	0,190963	-0,952607	0,199643	-1,58012	0,20029	-1,5417
500000	0,223156	-1,15002	0,235339	-1,93807	0,234827	-1,89995
600000	0,253501	-1,36085	0,269053	-2,30997	0,268285	-2,26984

800000	0,310466	-1,80283	0,332468	-3,07373	0,333689	-3,02722
1000000	0,367581	-2,25285	0,398137	-3,84585	0,405839	-3,79418

	Module 12		**Module 16**	
f(Hz)	**Re (ohm)**	**Im (ohm)**	**Re (ohm)**	**Im (ohm)**
20	117,539001	-5,74894	68,876404	-1,82309
25	117,307999	-7,16778	68,834198	-2,28676
30	117,058998	-8,59768	68,786102	-2,74786
40	116,453003	-11,3748	68,676804	-3,68685
50	115,734001	-14,1868	68,5383	-4,60623
60	114,870003	-16,8486	68,387299	-5,53442
80	112,907997	-22,0198	68,0327	-7,34145
100	110,504997	-26,8631	67,561302	-9,12257
120	107,736	-31,333599	67,016998	-10,8532
150	103,068001	-37,309299	66,037201	-13,3707
200	94,4356	-45,249802	64,029999	-17,2725
250	85,442703	-50,7924	61,642899	-20,7627
300	76,699997	-54,304798	58,9706	-23,7993
400	61,187901	-56,970901	53,158401	-28,5298
500	48,847698	-56,1441	47,229	-31,6
600	39,365299	-53,688	41,596001	-33,314
800	26,580299	-47,423199	31,969801	-33,988
1000	18,903999	-41,487099	24,683201	-32,6771
1200	14,0508	-36,493698	19,3288	-30,6049
2000	5,77995	-23,9727	8,59896	-22,4591
3000	2,77056	-16,543699	4,16138	-16,1223
5000	1,09127	-10,1446	1,59779	-10,0847
8000	0,473055	-6,40246	0,660899	-6,40527
10000	0,32363	-5,13588	0,43944	-5,14771
15000	0,171057	-3,43239	0,218339	-3,45452
20000	0,115852	-2,57368	0,141065	-2,60443
30000	0,077201	-1,70913	0,088	-1,7577
40000	0,065939	-1,27363	0,072326	-1,34049
50000	0,063247	-1,01069	0,06779	-1,09608
60000	0,063866	-0,834849	0,067671	-0,93869
80000	0,069679	-0,614402	0,072751	-0,75487
100000	0,077499	-0,482521	0,080741	-0,65956
120000	0,085921	-0,395853	0,089389	-0,60883
150000	0,099026	-0,310818	0,102521	-0,57844
200000	0,119732	-0,230989	0,123691	-0,58918
250000	0,139085	-0,189474	0,143818	-0,63795
300000	0,157214	-0,167416	0,162722	-0,70614
400000	0,190767	-0,154996	0,198803	-0,87391
500000	0,221708	-0,164066	0,233214	-1,06309
600000	0,251557	-0,184712	0,267213	-1,26442

800000	0,309726	-0,243355	0,335891	-1,68616
1000000	0,372604	-0,31139	0,411911	-2,12219

2 [B] Electroluminescence measurement pictures

Monocrystalline:

Module 1

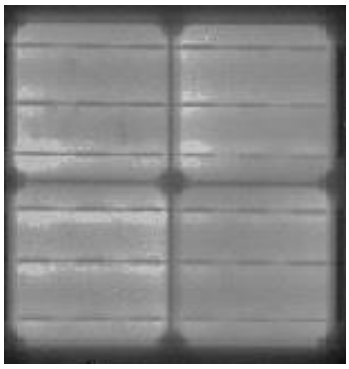

Module 2

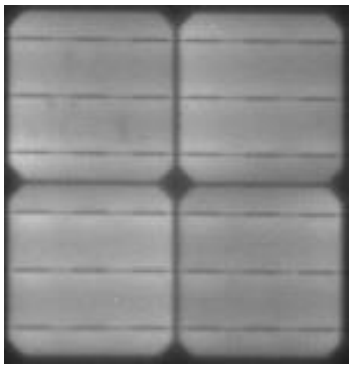

Module 3

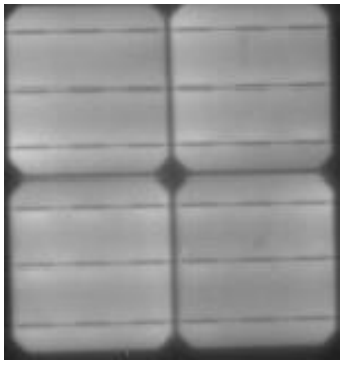

Module 4

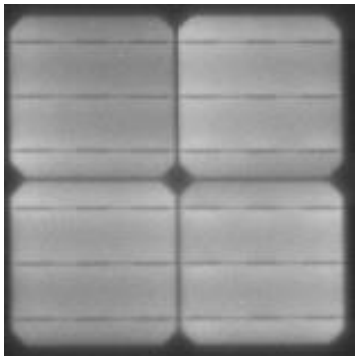

Module 7

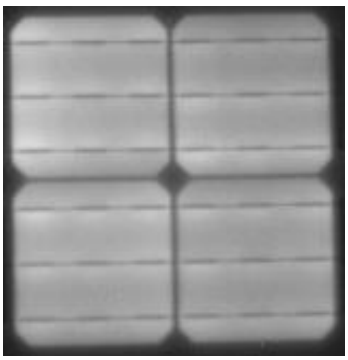

Module 8

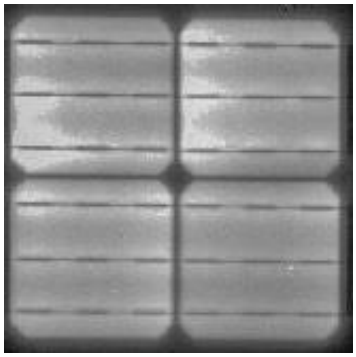

Module 9

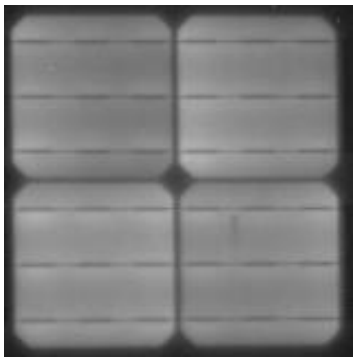

Module 10

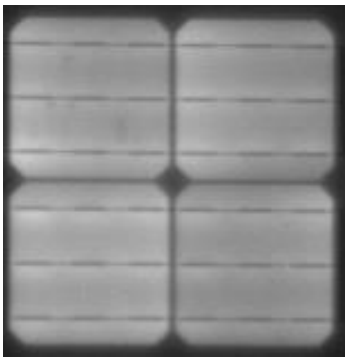

Multicrystalline:

Module 13

Module 14

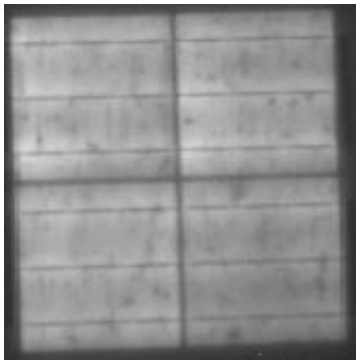

Module 15

Module 17

Module 18

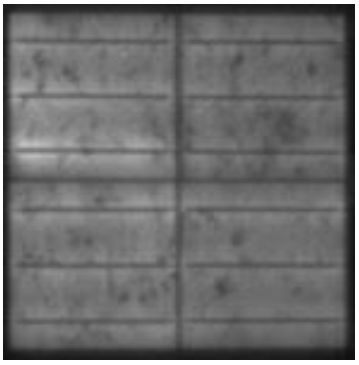

Module 19

Module 20

3 [C] Flash Tester measurement results

Producer	Phonosolar
Type	PS15M
Serial number	1_12R
Designation in LPVS	
Date of the laboratory measurement	27-04-17
Actual temperature	22.1 °C
The values are converter to the temperature	25 °C
G	1.0 kW/m^2
I_{SC}	8.942 A
V_{OC}	2.519 V
η	10.90 %
FF	68.43 %
P_{max}	15.413 W
V_{Pmax}	1.900 V
I_{Pmax}	8.111 A
R_s	0.1 Ω
R_p	9.4 Ω

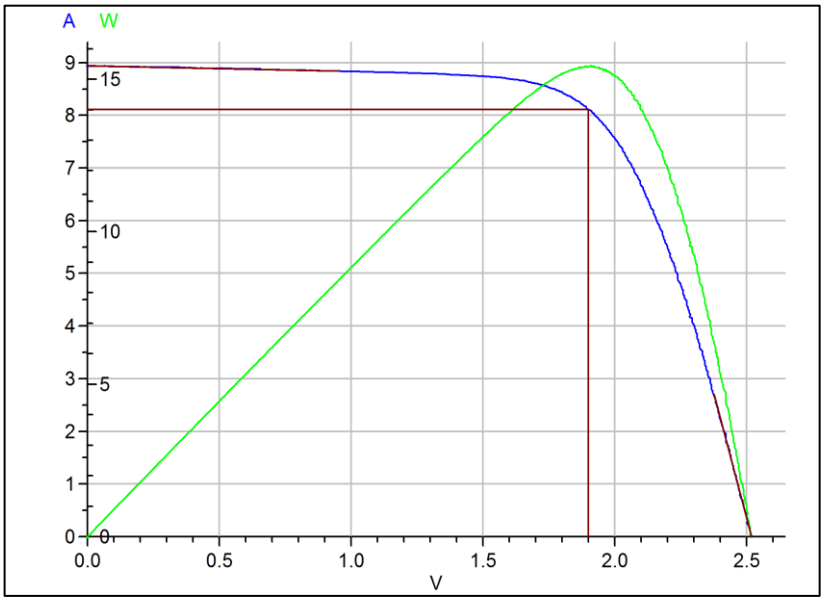

I-V and P-V diagrams for direct 1_12R.

Producer	Phonosolar
Type	PS15M
Serial number	1_12R_reverse
Designation in LPVS	
Date of the laboratory measurement	27-04-17
Actual temperature	22.1 °C
The values are converter to the temperature	25 °C
G	1.0 kW/m^2

I_{SC}	8.939 A
V_{OC}	2.398 V
η	10.95 %
FF	72.22 %
P_{max}	15.481 W
V_{Pmax}	1.896 V
I_{Pmax}	8.163 A
R_s	0.1 Ω
R_p	10.0 Ω

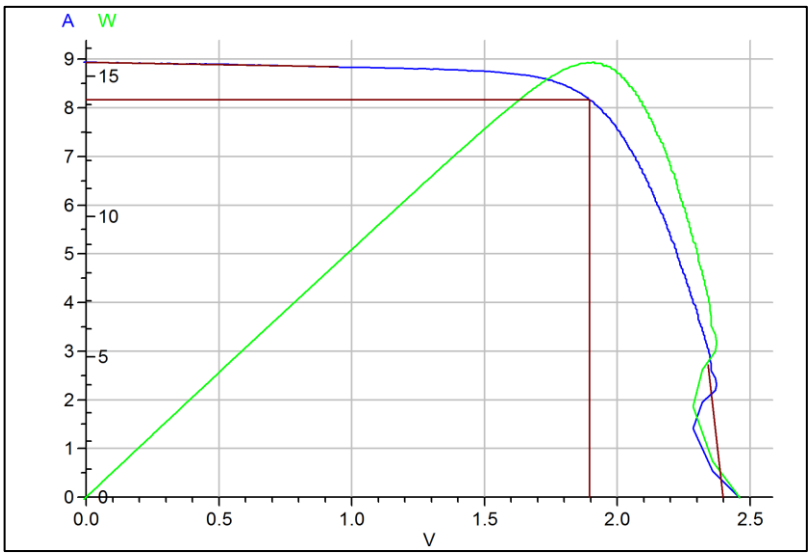

I-V and P-V diagrams for direct 1_12R_reverse.

Producer	Phonosolar
Type	PS15M
Serial number	1_22R
Designation in LPVS	
Date of the laboratory measurement	27-04-17
Actual temperature	22.2 °C
The values are converter to the temperature	25 °C
G	1.0 kW/m^2
I_{SC}	8.949 A
V_{OC}	2.522 V
η	11.01 %
FF	68.95 %
P_{max}	15.558 W
V_{Pmax}	1.901 V
I_{Pmax}	8.186 A
R_s	0.1 Ω
R_p	16.3 Ω

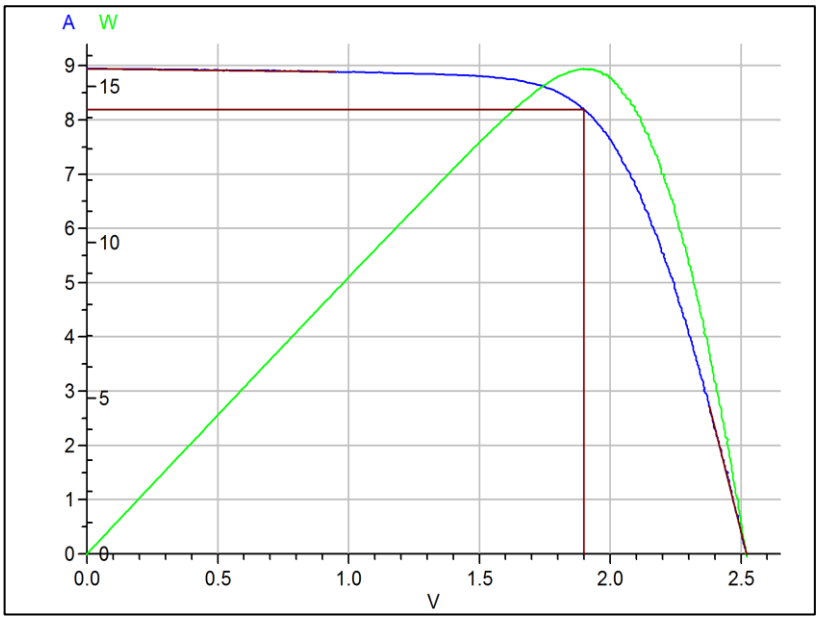

I-V and P-V diagrams for direct 1_22R.

Producer	Phonosolar
Type	PS15M
Serial number	1_22R_reverse
Designation in LPVS	
Date of the laboratory measurement	27-04-17
Actual temperature	22.1 °C
The values are converter to the temperature	25 °C
G	1.0 kW/m^2
I_{SC}	8.947 A
V_{OC}	2.402 V
η	11.05 %
FF	72.69 %
P_{max}	15.623 W
V_{Pmax}	1.898 V
I_{Pmax}	8.231 A
R_s	0.0 Ω
R_p	15.9 Ω

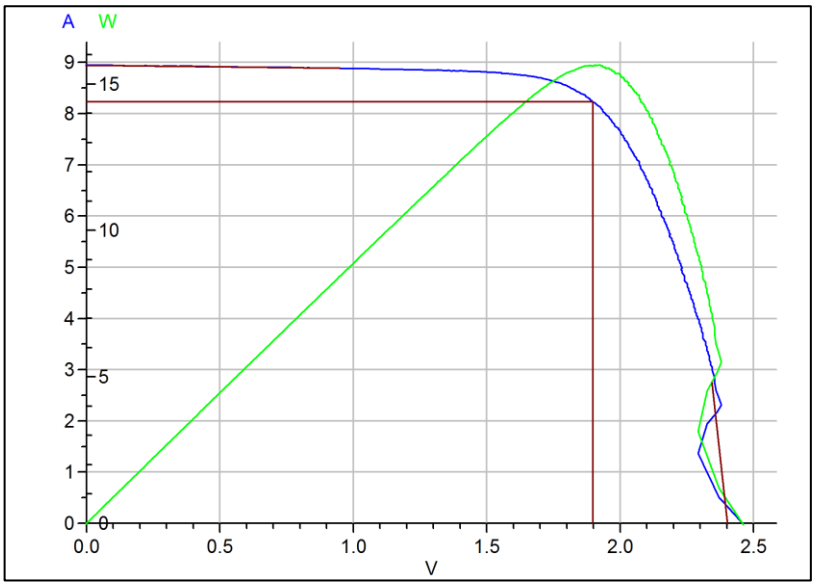

I-V and P-V diagrams for direct 1_22R_reverse.

Producer	Phonosolar
Type	PS15M
Serial number	1_33R
Designation in LPVS	
Date of the laboratory measurement	27-04-17
Actual temperature	22.2 °C
The values are converter to the temperature	25 °C
G	1.0 kW/m^2
I_{SC}	8.955 A
V_{OC}	2.523 V
η	11.04 %
FF	69.09 %
P_{max}	15.611 W
V_{Pmax}	1.902 V
I_{Pmax}	8.208 A
R_s	0.1 Ω
R_p	19.1 Ω

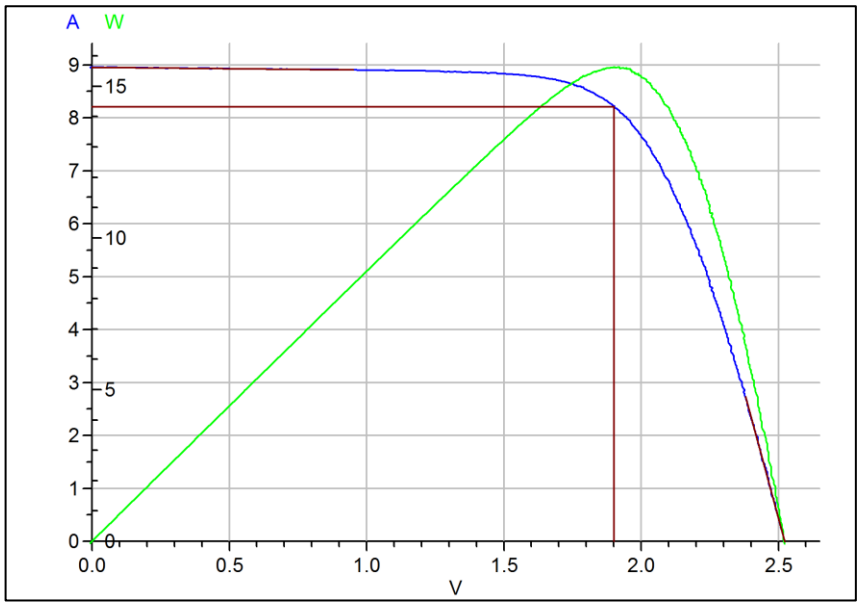

I-V and P-V diagrams for direct 1_33R.

Producer	Phonosolar
Type	PS15M
Serial number	1_33R_reverse
Designation in LPVS	
Date of the laboratory measurement	27-04-17
Actual temperature	22.2 °C
The values are converter to the temperature	25 °C
G	1.0 kW/m^2
I_{SC}	8.950 A
V_{OC}	2.423 V
η	11.09 %
FF	72.28 %
P_{max}	15.673 W
V_{Pmax}	1.898 V
I_{Pmax}	8.259 A
R_s	0.0 Ω
R_p	20.1 Ω

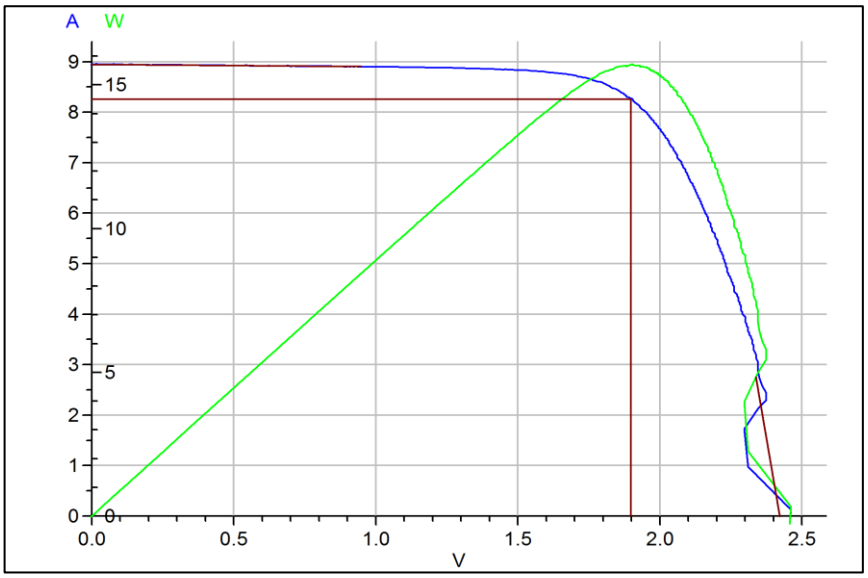

I-V and P-V diagrams for direct 1_33R_reverse.

Producer	Phonosolar
Type	PS15M
Serial number	1_82R_reverse
Designation in LPVS	
Date of the laboratory measurement	27-04-17
Actual temperature	22.2 °C
The values are converter to the temperature	25 °C
G	1.0 kW/m^2
I_{SC}	8.957 A
V_{OC}	2.414 V
η	11.14 %
FF	72.85 %
P_{max}	15.752 W
V_{Pmax}	1.899 V
I_{Pmax}	8.297 A
R_s	0.0 Ω
R_p	26.5 Ω

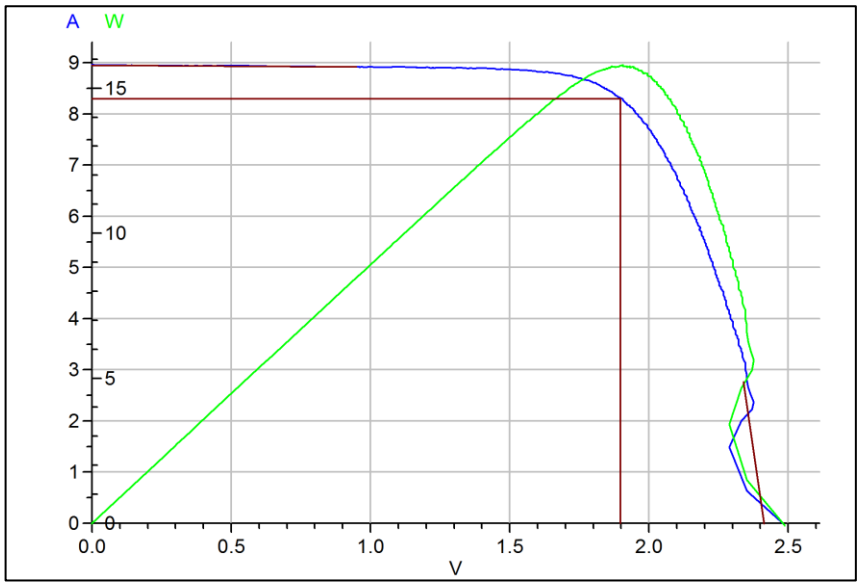

I-V and P-V diagrams for direct 1_82R_reverse.

Producer	Phonosolar
Type	PS15M
Serial number	1_330R
Designation in LPVS	
Date of the laboratory measurement	27-04-17
Actual temperature	22.2 °C
The values are converter to the temperature	25 °C
G	1.0 kW/m^2
I_{SC}	8.958 A
V_{OC}	2.525 V
η	11.12 %
FF	69.48 %
P_{max}	15.716 W
V_{Pmax}	1.903 V
I_{Pmax}	8.258 A
R_s	0.1 Ω
R_p	35.6 Ω

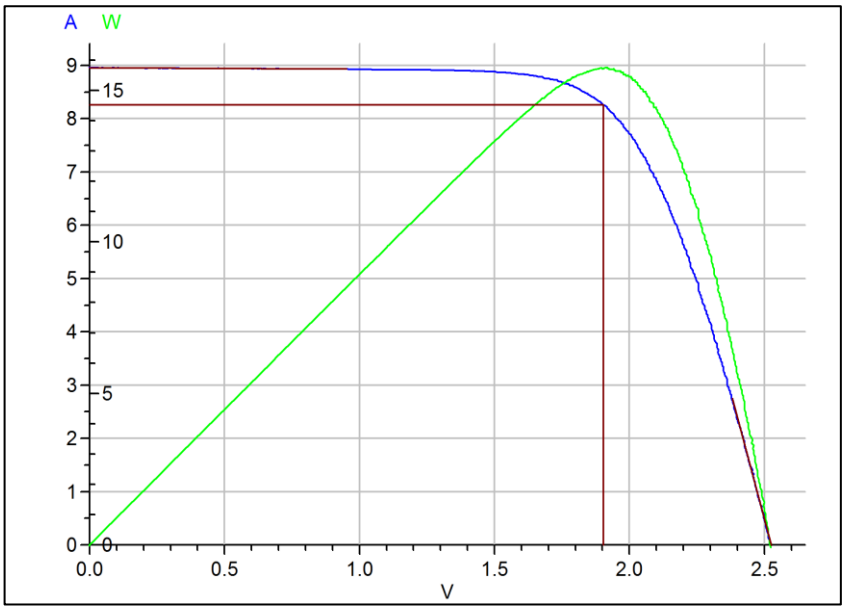

I-V and P-V diagrams for direct 1_330R.

Producer	Phonosolar
Type	PS15M
Serial number	1_330R_reverse
Designation in LPVS	
Date of the laboratory measurement	27-04-17
Actual temperature	22.2 °C
The values are converter to the temperature	25 °C
G	1.0 kW/m^2
I_{SC}	8.955 A
V_{OC}	2.413 V
η	11.16 %
FF	73.00 %
P_{max}	15.775 W
V_{Pmax}	1.898 V
I_{Pmax}	8.310 A
R_s	0.0 Ω
R_p	45.0 Ω

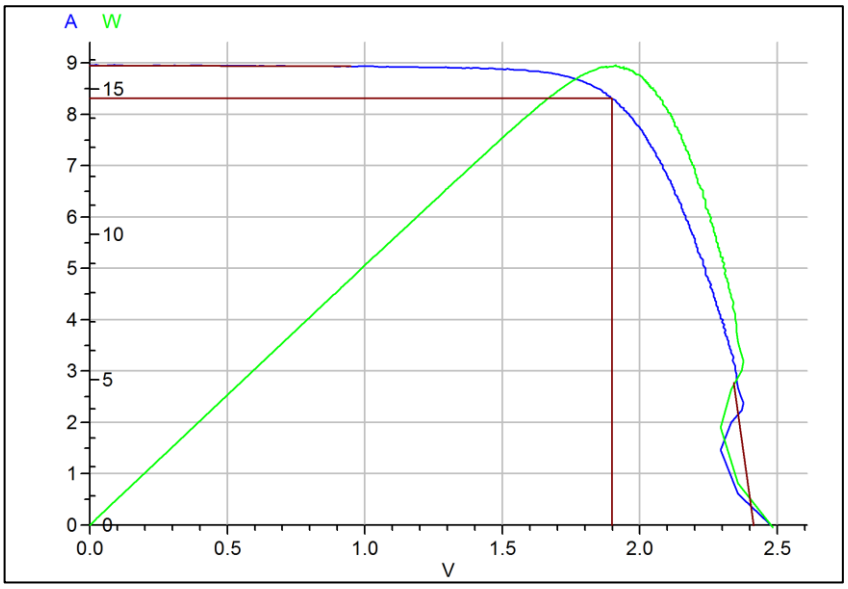

I-V and P-V diagrams for direct 1_330R_reverse.

Producer	Phonosolar
Type	PS15M
Serial number	1_680R
Designation in LPVS	
Date of the laboratory measurement	27-04-17
Actual temperature	22.3 °C
The values are converter to the temperature	25 °C
G	1.0 kW/m^2
I_{SC}	8.960 A
V_{OC}	2.525 V
η	11.13 %
FF	69.54 %
P_{max}	15.735 W
V_{Pmax}	1.906 V
I_{Pmax}	8.256 A
R_s	0.1 Ω
R_p	45.5 Ω

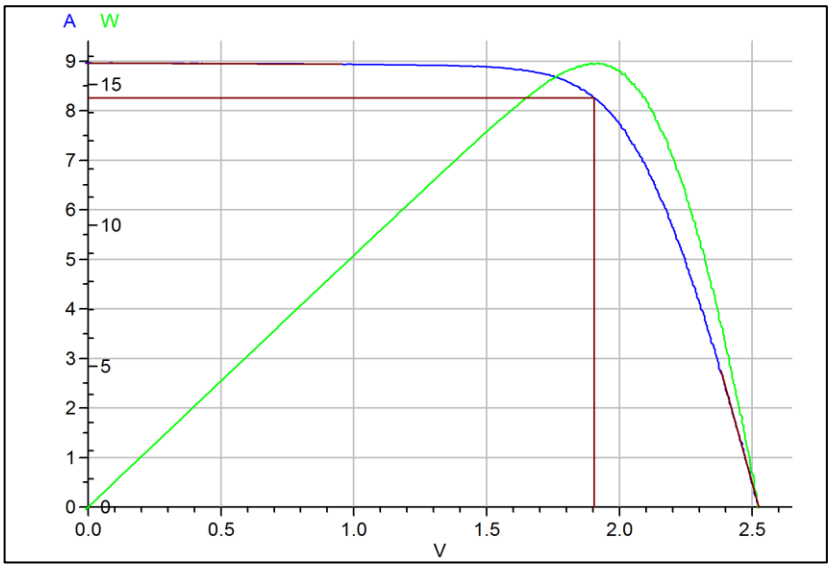

I-V and P-V diagrams for direct 1_680R.

Producer	Phonosolar
Type	PS15M
Serial number	1_680R_reverse
Designation in LPVS	
Date of the laboratory measurement	27-04-17
Actual temperature	22.3 °C
The values are converter to the temperature	25 °C
G	1.0 kW/m^2
I_{SC}	8.960 A
V_{OC}	2.406 V
η	11.17 %
FF	73.25 %
P_{max}	15.788 W
V_{Pmax}	1.899 V
I_{Pmax}	8.314 A
R_s	0.0 Ω
R_p	43.5 Ω

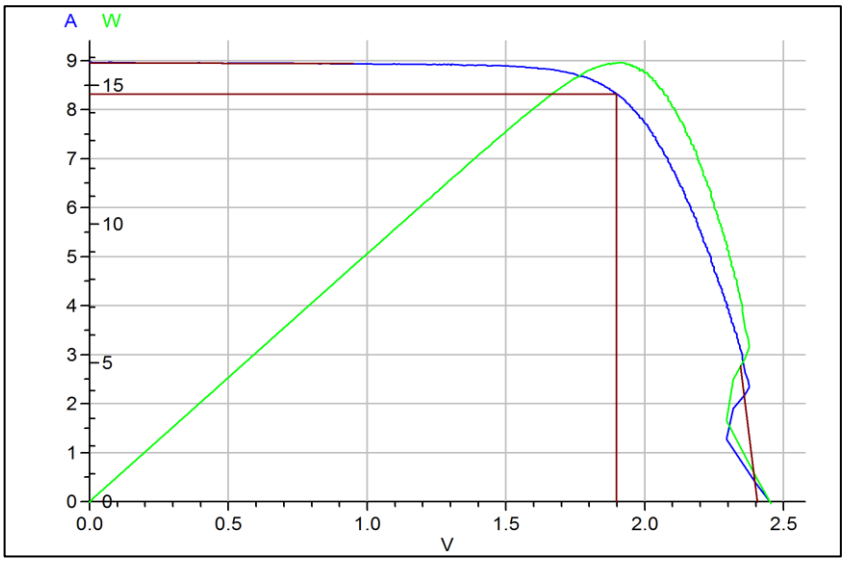

I-V and P-V diagrams for direct 1_680R_reverse.

Producer	Phonosolar
Type	PS15M
Serial number	1_820R
Designation in LPVS	
Date of the laboratory measurement	27-04-17
Actual temperature	22.2 °C
The values are converter to the temperature	25 °C
G	1.0 kW/m^2
I_{SC}	8.959 A
V_{OC}	2.523 V
η	11.12 %
FF	69.57 %
P_{max}	15.727 W
V_{Pmax}	1.904 V
I_{Pmax}	8.258 A
R_s	0.1 Ω
R_p	46.1 Ω

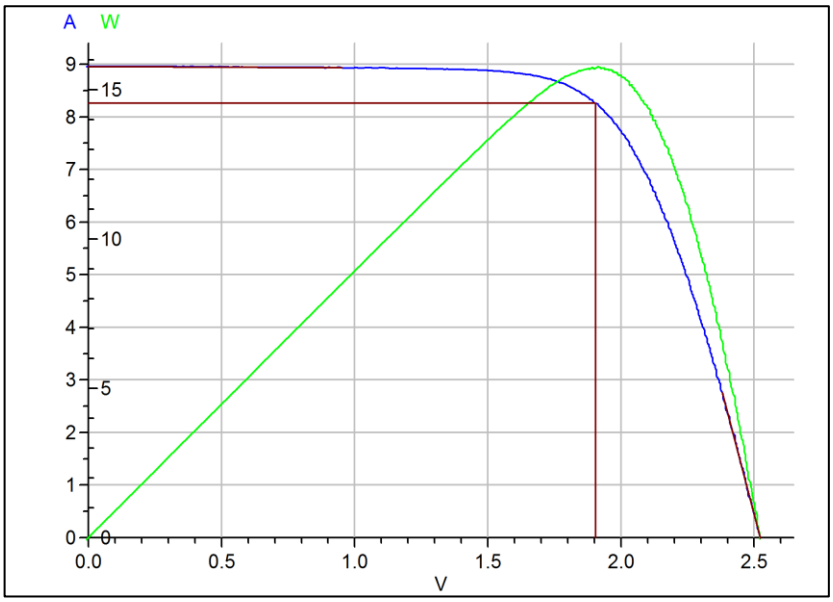

I-V and P-V diagrams for direct 1_820R.

Producer	Phonosolar
Type	PS15M
Serial number	1_820R_reverse
Designation in LPVS	
Date of the laboratory measurement	27-04-17
Actual temperature	22.2 °C
The values are converter to the temperature	25 °C
G	1.0 kW/m^2
I_{SC}	8.959 A
V_{OC}	2.407 V
η	11.16 %
FF	73.16 %
P_{max}	15.778 W
V_{Pmax}	1.899 V
I_{Pmax}	8.309 A
R_s	0.0 Ω
R_p	44.3 Ω

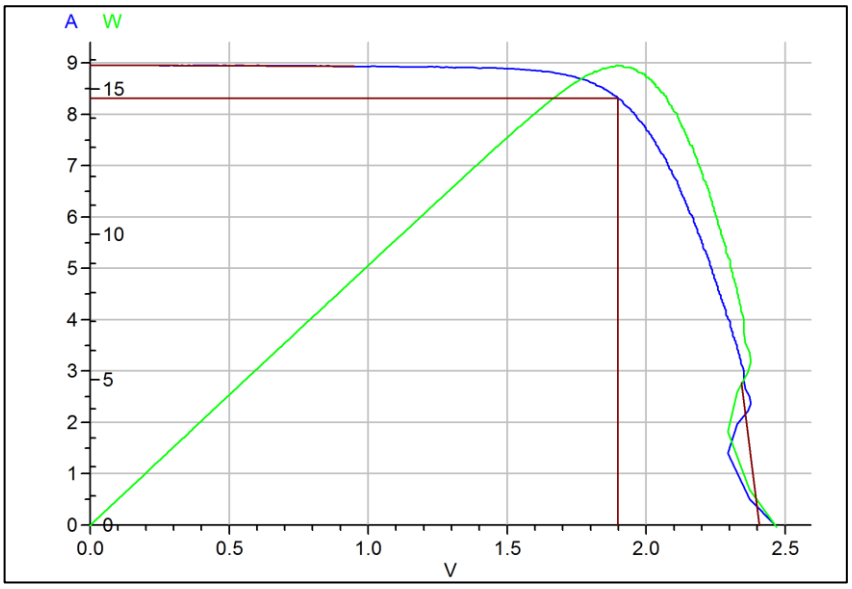

I-V and P-V diagrams for direct 1_820R_reverse.

Producer	Phonosolar
Type	PS15M
Serial number	1_18K
Designation in LPVS	
Date of the laboratory measurement	27-04-17
Actual temperature	22.2 °C
The values are converter to the temperature	25 °C
G	1.0 kW/m^2
I_{SC}	8.959 A
V_{OC}	2.524 V
η	11.13 %
FF	69.56 %
P_{max}	15.733 W
V_{Pmax}	1.902 V
I_{Pmax}	8.270 A
R_s	0.1 Ω
R_p	55.5 Ω

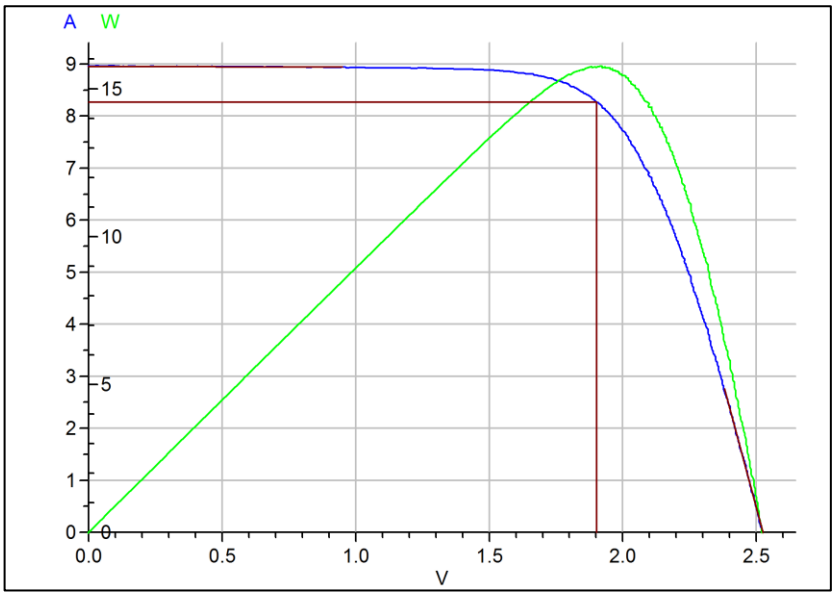

I-V and P-V diagrams for direct 1_18K.

Producer	Phonosolar
Type	PS15M
Serial number	1_18K_reverse
Designation in LPVS	
Date of the laboratory measurement	27-04-17
Actual temperature	22.3 °C
The values are converter to the temperature	25 °C
G	1.0 kW/m^2
I_{SC}	8.958 A
V_{OC}	2.437 V
η	11.18 %
FF	72.38 %
P_{max}	15.800 W
V_{Pmax}	1.900 V
I_{Pmax}	8.317 A
R_s	0.0 Ω
R_p	61.2 Ω

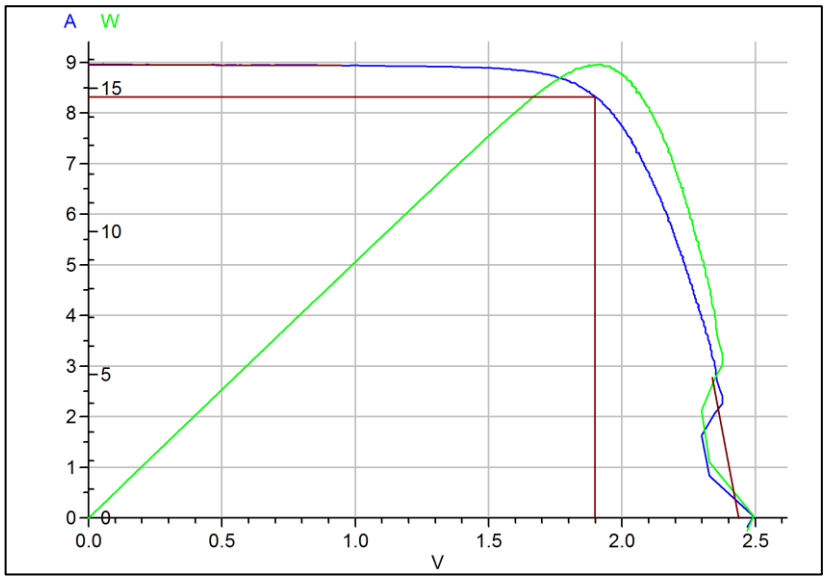

I-V and P-V diagrams for direct 1_18K_reverse.

Producer	Phonosolar
Type	PS15M
Serial number	1_390K
Designation in LPVS	
Date of the laboratory measurement	27-04-17
Actual temperature	22.3 °C
The values are converter to the temperature	25 °C
G	1.0 kW/m^2
I_{SC}	8.962 A
V_{OC}	2.524 V
η	11.13 %
FF	69.55 %
P_{max}	15.735 W
V_{Pmax}	1.905 V
I_{Pmax}	8.262 A
R_s	0.1 Ω
R_p	46.8 Ω

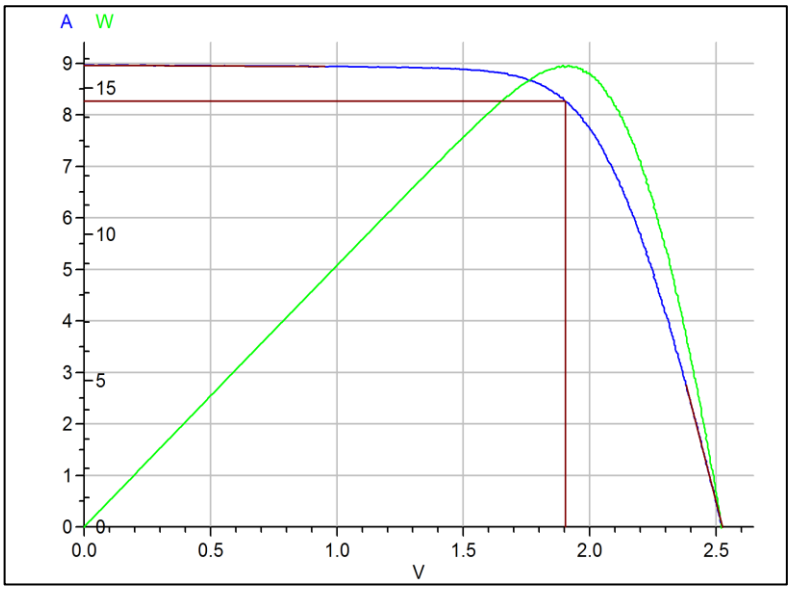

I-V and P-V diagrams for direct 1_390K.

Producer	Phonosolar
Type	PS15M
Serial number	1_390K_reverse
Designation in LPVS	
Date of the laboratory measurement	27-04-17
Actual temperature	22.3 °C
The values are converter to the temperature	25 °C
G	1.0 kW/m^2
I_{SC}	8.957 A
V_{OC}	2.422 V
η	11.17 %
FF	72.79 %
P_{max}	15.794 W
V_{Pmax}	1.900 V
I_{Pmax}	8.313 A
R_s	0.0 Ω
R_p	58.7 Ω

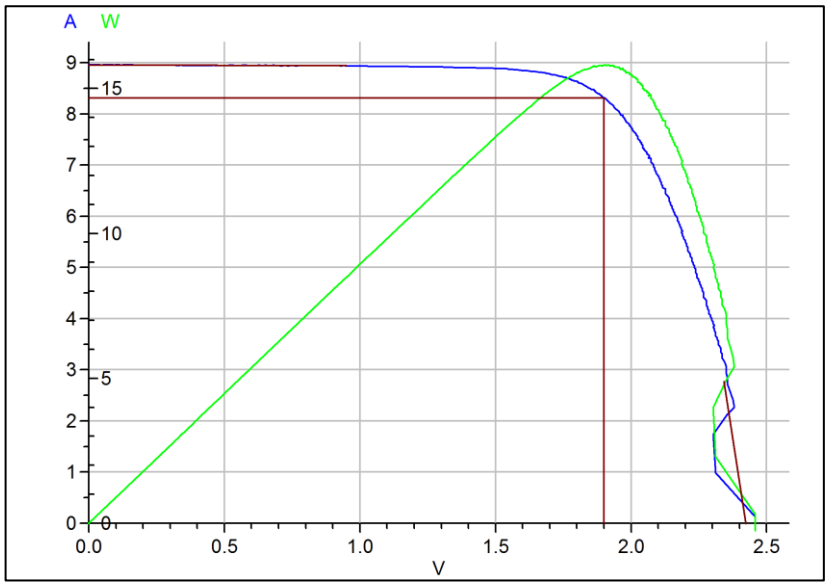

I-V and P-V diagrams for direct 1_390K_reverse.

4 [D] The values for plotting the I-V and P-V curves for PV panels 1_56R, 1_180R and 1_27K.

1_56R			1_180R		
voltage[V]	current[A]	power[W]	voltage[V]	current[A]	power[W]
0,004	8,956	0,033	0,004	8,952	0,037
0,126	8,951	1,125	0,126	8,947	1,129
0,209	8,951	1,868	0,209	8,947	1,871
0,345	8,946	3,09	0,341	8,947	3,051
0,513	8,932	4,747	0,531	8,942	4,752
0,644	8,927	5,747	0,644	8,942	5,756
0,839	8,922	7,487	0,834	8,932	7,451
1,001	8,904	8,91	1	8,922	8,924
1,303	8,885	11,58	1,298	8,903	11,556
1,528	8,846	13,516	1,528	8,869	13,547
1,67	8,754	14,62	1,664	8,786	14,622
1,851	8,422	15,587	1,845	8,463	15,614
2,031	7,465	15,164	2,03	7,511	15,251
2,212	5,414	11,976	2,212	5,457	12,068
2,305	4,052	9,339	2,299	4,094	9,415
2,398	2,368	5,679	2,398	2,411	5,781
2,437	1,602	3,904	2,442	1,644	4,015
2,501	0,459	1,148	2,501	0,474	1,185
2,545	-0,512	-1,304	2,545	-0,516	-1,314
2,545	-0,527	-1,341	2,545	-0,539	-1,373

1_27K		
voltage[V]	**current[A]**	**power[W]**
0	8,961	0,001
0,132	8,956	1,182
0,215	8,956	1,925
0,347	8,951	3,104
0,537	8,951	4,809
0,645	8,951	5,77
0,84	8,938	7,511
1,006	8,933	8,99
1,304	8,918	11,632
1,534	8,87	13,609
1,676	8,787	14,726
1,852	8,455	15,656
2,033	7,48	15,205
2,218	5,419	12,022
2,307	4,053	9,35
2,399	2,384	5,719
2,443	1,617	3,951
2,501	0,463	1,159
2,546	-0,522	-1,328
2,545	-0,528	-1,343

5 [E] The values for plotting temperature dependent I-V curves of c-Si.

	25°C		**45°C**		**65°C**	
load	**voltage[V]**	**current[A]**	**voltage[V]**	**current[A]**	**voltage[V]**	**current[A]**
0	0,06	1,13	0,2	1,15	0,11	1,21
0,1	0,28	1,13	0,32	1,14	0,26	1,19
0,2	0,41	1,07	0,41	1,02	0,36	1,05
0,3	0,46	0,92	0,44	0,84	0,4	0,86
0,4	0,48	0,79	0,455	0,72	0,412	0,7
0,5	0,49	0,68	0,463	0,61	0,42	0,59
0,6	0,5	0,59	0,467	0,51	0,426	0,52
0,7	0,51	0,5	0,47	0,43	0,43	0,45
0,8	0,51	0,49	0,475	0,38	0,435	0,39
0,9	0,515	0,42	0,48	0,31	0,438	0,35
1	0,52	0,34	0,484	0,27	0,446	0,27
2	0,526	0,24	0,487	0,22	0,45	0,2
3	0,53	0,16	0,492	0,15	0,455	0,12
4	0,53	0,08	0,496	0,08	0,457	0,06
infinity	0,53	0	0,5	0	0,46	0

6 [F] The values for plotting illumination dependent I-V curves of c-Si.

	45cm		35cm		30cm	
load	**voltage[V]**	**current[A]**	**voltage[V]**	**current[A]**	**voltage[V]**	**current[A]**
0	0,07	1,001	0,09	1,435	0,13	1,773
0,1	0,17	0,994	0,28	1,428	0,3	1,763
0,2	0,27	0,973	0,37	1,392	0,45	1,676
0,3	0,37	0,971	0,47	1,281	0,51	1,371
0,4	0,43	0,928	0,5	1,092	0,53	1,128
0,5	0,48	0,849	0,52	0,923	0,54	0,941
0,6	0,51	0,755	0,53	0,799	0,545	0,807
0,7	0,52	0,675	0,538	0,704	0,55	0,705
0,8	0,525	0,606	0,542	0,628	0,55	0,628
0,9	0,53	0,52	0,55	0,568	0,55	0,571
1	0,54	0,4	0,55	0,516	0,554	0,44
2	0,548	0,266	0,56	0,271	0,56	0,3
3	0,55	0,18	0,56	0,183	0,562	0,19
4	0,555	0,1	0,56	0,139	0,566	0,11
infinity	0,56	0	0,56	0	0,57	0

7 [G] The list of figures.